NTNU
Norwegian University of Science and Technology

Faculty of Natural Sciences and Technology
Department of Chemical Engineering

DIPLOMA WORK 2009

Title: Optimal operation of a LNG process	**Subject (3-4 words): Cooling cycles, LNG, optimization.**
Author: Luber Perez	**Carried out through:** January 13rd – June 2nd
Advisor: Prof. Sigurd Skogestad **Co-advisor:** Ph.D. stip. Magnus Glosli Jacobsen	**Number of pages** **Main report: 50** **Apendix: 2**

ABSTRACT

Goal of work (key words): The main goal of the diploma thesis is the optimization of a liquefied natural gas (LNG) process, the PRICO process. The work is divided into two sections; first, it is taken in account the design of the process and then the optimal operation in steady state is carried out. In the first section of the work, the HYSYS simulator was used to build nine different design cases of the PRICO process and the results were compared with the data reported. The second section consisted of determining the optimal conditions for the PRICO process in two different modes: The production of LNG is a specification and it is tried to minimize the compressor work (Mode I) and when the compressor work is set and the goal is to maximize the LNG production (Mode II). Once the optimal conditions for both modes were found, some disturbances were introduced into the system. The process was re-optimized and the effect of the disturbances over the system was studied.

Conclusions and recommendations (key words): In the design part of the work, the results matched the data reported in a previous work. An interesting task could be to use HYSYS to optimize the process design. In the operation part, it was found a new value for heat exchange area. For both Modes I and II the optimum nominal point was stable for natural gas temperature disturbances. The Mode II resulted to be stable for composition refrigerant disturbances. Thus, it would be interesting to do all the disturbance study for Mode II but using the MR composition of Mode I.

I declare that this is an independent work according to the exam regulations
of the Norwegian University of Science and Technology

Date and signature: .....

Acknowledgements

First of all, I would like to thank Prof. Sigurd Skogestad who gave me the great opportunity of working on this thesis which represents the end of my studies of chemical engineering and the beginning of new times. Thanks to Ph.D. student Magnus Jacobsen for being so helpful, patient and for his important guidance during these months of hard work.

I want to thanks my flat mate Matt who helped me with the writing of the thesis. I really appreciate that he accepted to help me without any complain or request. Gracias amigo!

Gracias a Andrea, for her support and good humor, always making me laugh and to get relax during the hard working days, gracias Che!

I would also like to thank the people in the international office in Venezuela who gave me the chance to participate in the exchange program between my home university and the NTNU.

My acknowledgement also goes to my parents Carlos and Luzmila, and to my family for their incredible support, helping me to walk this long road fill with obstacles and stumbles. Without them nothing of that would be possible.

Contents

Acknowledgements **2**
Contents **3**
1 Introduction **4**
2 Background **6**
2.1 Introduction to cooling cycles 6
2.2 Liquefaction of natural gas 8
2.3 Degrees of freedom 10
2.4 Characteristic compressor curves 11
2.5 Introduction to numerical optimization 13
2.5.1 Optimization methods 13
3 Design **15**
3.1 Process description 15
3.2 HYSYS modeling 16
3.3 Results for design 18
3.4 Conclusions 23
3.5 Further work 24
4 Optimal operation **25**
4.1 Process description 25
4.1.1 Nominal conditions 26
4.1.2 Degrees of freedom 27
4.2 HYSYS modeling 28
4.2.1 Compressor model 28
4.3 Solving optimization problem 30
4.3.1 Optimization in HYSYS 31
4.4 Nominal optimum 32
4.4.1 UA values for optimization 32
4.4.2 Mode I: Nominal optimum for given production 32
4.4.3 Mode II: Nominal optimum for given power 34
4.4.4 Nominal optimum refrigerant composition 35
4.5 Optimal operation with disturbances 36
4.5.1 Mode I 36
4.5.2 Mode II 42
4.6 Conclusions 47
4.7 Future work 48
References **49**
Nomenclature **50**
Appendix **52**
A.1 Refrigerant composition reported by Jensen for 9 different design cases. 52
A.2 Optimal refrigerant compositions reported by Jensen for operation. 53

1 Introduction

It is well known that the worldwide energy demand has rapidly increased during the recent years and the available resources are becoming insufficient. Oil is no longer the preferred energy resource and other resources have become more viable as a replacement for it. Natural gas has become one of the most important ways to obtain energy and its consumption could increase from 104 trillion cubic feet in 2005 to 158 trillion cubic feet in 2030 [1]. As natural gas produces less carbon dioxide than either coal or petroleum when it is burned, national and regional plans implemented by governments to reduce greenhouse gas emissions may encourage its use to displace other fossil fuels as well.

Norway is the second largest exporter of gas to Europe, only Russia is larger. In 2006, Norway accounted for 30 percent of all gas production in Western Europe. On a world basis, Norway ranks as the fifth largest producer and the third largest exporter, despite the fact that it has only 1.6 percent of the world's proven gas reserves. As of today, Norway has exported more than 1100 billion Sm^3 of gas. Of the total expected recoverable resources of 6000 billion sm^3, only about 20 percent has been produced [2].

In situations where the gas market is far away from the source of the natural gas, it is a more economic solution to transport the gas as liquefied natural gas (LNG) instead of in a natural gas pipe line. LNG is natural gas (mainly methane) that has been cooled and condensed to a liquid about -160 °C at atmospheric pressure. The great advantage of transporting natural gas as LNG is that the natural gas reduces 600 times its volume and consequently large amounts can be transported.

There are several natural gas liquefaction processes used in the industry such as, pure fluid cascade process, mixed fluid refrigerant and mixed fluid cascade process. This paper studies a simple cooling cycle known as the PRICO process which uses a mixed fluid refrigerant. The PRICO process was developed and marketed by Black and Veatch Company, and it has several key advantages. The advantages include the lowest capital costs of all competing technologies, a simplified refrigeration system requiring minimal equipment and simplified control and flexibility in feed gas composition [3].

In order to reduce the investment costs of a plant, much effort is put to find the optimal design of the process. This work tries to validate the data design found in earlier work done by Jørgen B. Jensen [4]. The main point is to see if the previous data found using the gPROMS software can be reproduced using the HYSYS simulator instead. Specifically, it is compared the area required for NG-HX in nine different cases. Each case varies the specifications of the model, such as production of flash gas, compressor power, compression pressure and so forth.

An extensive study of the steady state operation of the process is also included in the thesis. In this part of the work, it is sought to determine the optimal conditions for the PRICO process in two different modes:

- **Mode I:** Minimize the compressor work for a given production rate of LNG.

- **Mode II:** Maximize production of LNG for a given compressor work.

After finding the optimal conditions for both modes, some disturbances (compressor work, NG pressure, NG and MR temperatures, NG feed rate) were introduced and the process was re-optimized to find new optimal conditions.

2 Background

2.1 Introduction to cooling cycles

A refrigeration system removes thermal energy from a low-temperature region and transfers heat to a high-temperature region. The most common refrigeration cycle is the vapor compression cycle, which is used in most household refrigerators as well as in many large commercial and industrial refrigeration systems. This process has four principal components: evaporator, compressor, condenser, and expansion (or throttle) valve.

The simple process is sketched in Fig 2.1 (taken from [4]), and also it is represented in a pressure enthalpy diagram, Fig. 2.2:

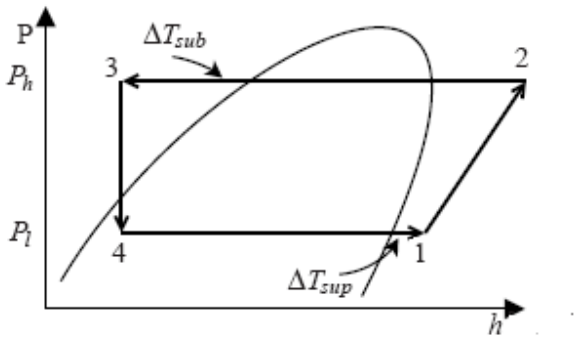

Figure 2.1: Pressure-enthalpy diagram for a simple refrigeration cycle

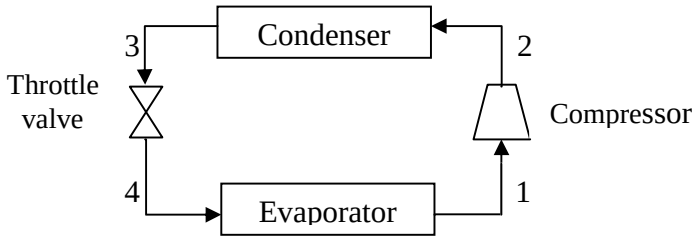

Figure 2.2: Simple refrigeration cycle of vapor compression

In step 4 to 1, heat is removed from the system to being refrigerated by the evaporation of the working fluid at low pressure (P_L). The saturated vapor at P_l is then compressed to high pressure (P_h), step 1 to 2. In step 2 to 3, the substance is de-superheated and then condensed to saturated liquid at constant pressure. During this process, the working substance rejects most of its energy to the condenser cooling water. The cycle is closed by an irreversible throttling process in which the temperature and pressure decrease at constant enthalpy.

In order to prevent liquid fed into the compressor, the vapor must be slightly superheated, ΔT_{sup}, at the outlet of the evaporator. The degree of superheating, ΔT_{sup}, *stands for the temperature difference between the evaporator outlet temperature and the saturation temperature at given pressure.*

The refrigerant is sub-cooled at the outlet of the condenser, as we can see in fig 2. The degree of sub-cooling (ΔT_{sub}) *represents the temperature difference between the condenser outlet temperature and the saturation temperature at given pressure.* However, sub-cooled liquid is normally unlike [4].

The traditional measure for the refrigeration cycle efficiency is the COP, coefficient of performance, and it is define as:

$$COP = \frac{|Q_L|}{W_s} \tag{2.1}$$

where Q_L is the heat removed from the system being refrigerated and W_s the power required by the compressor.

The COP is restricted by the efficiency of Carnot, which is the theoretical 'minimum fraction of the cooling duty Q_L that must be added as mechanical work *Ws'* [4]*:*

$$COP_{carnot} = \frac{|Q_L|}{W_s} = \frac{T_L}{T_H - T_L} \tag{2.2}$$

Since, the Carnot efficiency results from the assumption of an ideal reversible process neglecting world items like frictional pressure drop in the system or slight internal irreversibility during the compression of the refrigerant vapor a real process, such efficiency cannot be achieved in a real process.

Some improvement of the cycle efficiency could be gained by replacing the isenthalpic throttling step with an isentropic expansion. While such an improvement is theoretically possible and is therefore appealing, usually practical considerations have to be taken into account. In the practice, liquids tend to become vapor during the expansion step, which affects the safety of the turbine. In order to avoid vapor formation in the liquid turbine, a combination of a liquid turbine and a valve is used to be employed. The difference between these three expansion ways is shown in a Pressure-enthalpy diagram (taken from [4]), Fig. 2.3:

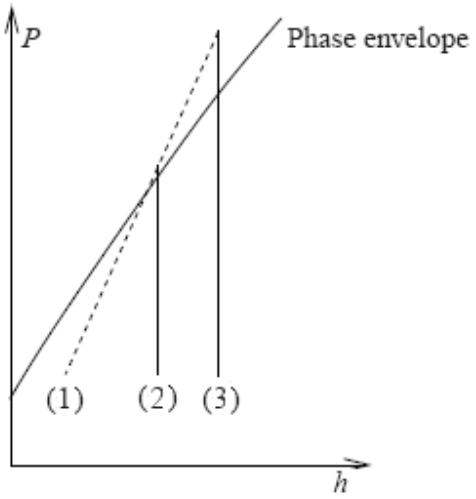

Figure 2.3: Three different ways for expansion: Liquid turbine (1), combination of turbine and valve (2), and expansion only with valve (3).

2.2 Liquefaction of natural gas

Liquefied natural gas (LNG) is natural gas that has been cooled to the point that condenses to a liquid, which occurs at a temperature of approximately -161 °C, at atmospheric pressure. The liquefaction process reduces the volume of gas by approximately 600 times, thus it is more economical to store natural gas where other forms of storage do not exist, and to transport gas over long distances for which pipelines are too expensive or for which other constraints exist. This last reason is which makes the LNG so important. Fig. 2.4 shows the cost of natural gas transportation for different transportation ways [5]. Liquefaction makes possible to move natural gas between continents in specially designed ships. Thus, LNG technology makes natural gas available throughout the world.

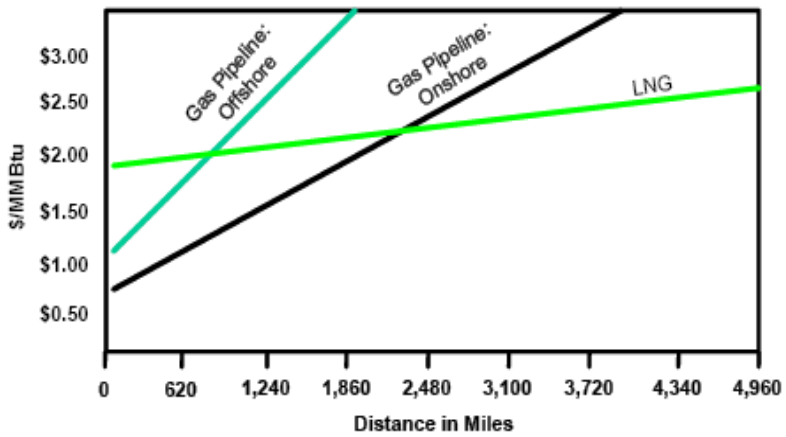

Figure 2.4: Natural transportation technology and cost relative to distance

In order to deliver natural gas from the field to the costumers, some different stages have to be done. These stages are known as the gas value chain:

- **Exploration** to find natural gas: Most of the time natural gas is discovered during the search for oil.

- **Liquefaction** to convert natural gas into a liquid state so that it can be transported in ships.

- **Shipping** the LNG in special purpose vessels.

- **Storage** of LNG in specially made tanks and **re-gasification** to convert the LNG from the liquid phase to the gaseous phase, ready to be moved to the final destination through the natural gas pipeline system.

A mechanical refrigeration process is used for the liquefaction of natural gas, where natural gas is cooled and liquefied by heat exchange with a separate refrigerant. In the last four decades, several licensed processes have been developed based upon this fundamental principle.. The main objective of these technological innovations (besides reducing unit investment and operation costs) is to optimize the efficiency of the refrigeration process employed in order to, in most cases, increase the LNG production. A liquefaction plant may consist of several parallel units (“trains”).

The indicative cooling curve of a natural gas, shown in Fig 2.5, profiles two different routes to liquefaction with pure and mixed refrigerants. For commercial liquefaction processes, the intent is to minimize the difference between the refrigerant curve and the natural gas cooling curve in order to produce higher volumes of LNG, taking into consideration plant availability and equipment reliability. The different technologies for LNG can be grouped as:

- Pure Refrigerant Process:

    - Cascade process: Uses three refrigeration circuits with propane, ethylene and (mostly) methane as refrigerant.

- Mixed Refrigerant Processes:

    - Single mixed refrigeration process (PRICO): Uses one main heat exchanger where both the natural gas and the mixed refrigerant are cooled by the cold refrigerant.

    - Dual Mixed Refrigerant process: Employs two parallel spiral wound cryogenic heat exchangers.

    - Mixed Refrigerant with Propane Pre-cooling and Nitrogen Sub-cooling: the natural gas and the mixed refrigerant are both pre-cooled before going to the main heat exchanger.

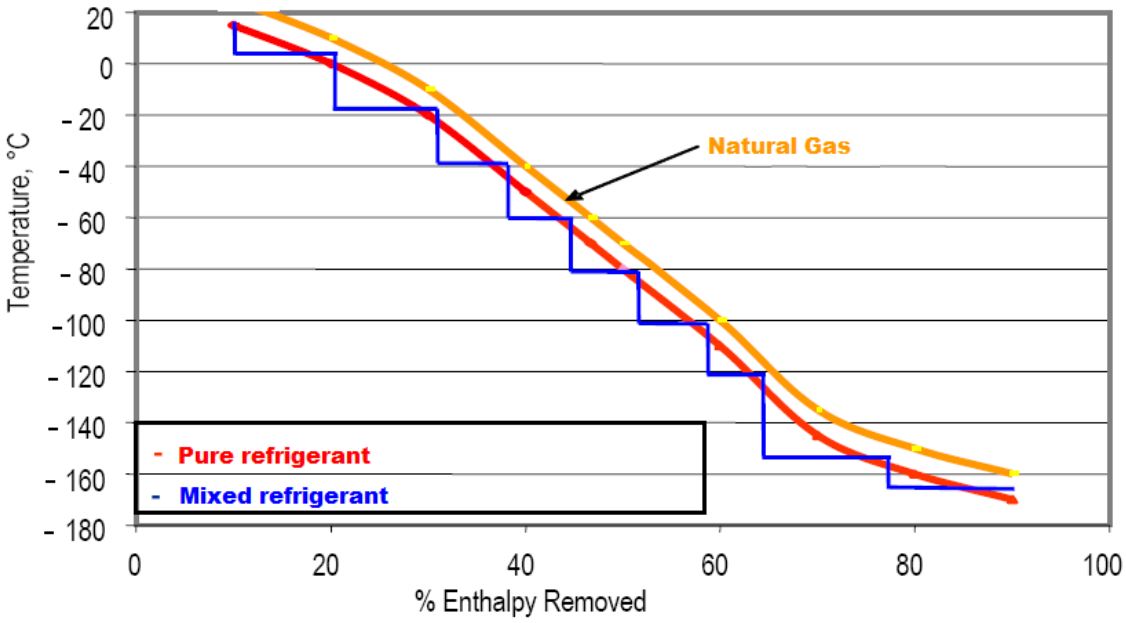

Figure 2.5: Cooling curves for pure and mixed refrigerant.

2.3 Degrees of freedom

One of the central problems in developing a steady-state process flowsheet is finding the number of variables that must be specified to completely define the process. This number is called the *design degrees of freedom* (N_{DOF}). In principle, the design degrees of freedom are easily calculated by simply subtracting the number of equations from the number of variables:

$$N_{DOF} = N_{MV} - N_{SV} \tag{2.3}$$

Where:
N_{MV} are the number of manipulated variables
N_{SV} are the number of specified variables

Once the design degrees of freedom have been found, the number of *optimization degrees of freedom* can be calculated by subtracting all variables that are set by specifications on production rate, product qualities, safety constraints, etc. Since in optimization some variables have to be controlled, there will be a reduction in the degrees of freedom. The optimization variables are the available degrees of freedom for maximizing some appropriate measure of profitability. Typical design optimization variables are reactor sizes, number of reactors, number of column trays, recycle flow rates, etc.

2.4 Characteristic compressor curves

During operation it is common to model the performance of the equipments like compressors, turbines, pumps, etc. The performance of these equipments is likely based by characteristics curves that link variables like flowrate, efficiency, rotational speed and so on; such curves are generally provided by the vendor of the equipment.

Normally the characteristic curves for compressor rating relate issues like reduce flowrate ($\dot{m}_r$), reduce rotational speed (Nr), pressure ratio (Pr) and compressor isentropic efficiency (Π). We can express the pressure ratio and the compressor efficiency as functions of the reduce flowrate and reduce rotational speed. Thus, the following dependencies can be used to study the steady state behavior of the compressor [4]:

$$Pr = f(\dot{m}_r, Nr) \tag{2.4}$$

$$\Pi = f(\dot{m}_r, N_r) \tag{2.5}$$

where:

$$\dot{m}r = \frac{\dot{m}\sqrt{\hat{R}T_1}}{D^2 P_1} \tag{2.6}$$

$$Nr = \frac{ND}{\sqrt{\hat{R}T_1}} \tag{2.7}$$

$\hat{R}$ (R/MW): Specific universal gas constant [$J \cdot Kg^{-1} \cdot K^{-1}$]
T_1: Compressor inlet temperature [K]
P_1: Compressor inlet pressure [$Kg \cdot m \cdot s^2$]
D: Compressor wheel diameter [m]
N: Rotational speed [s^{-1}]

Jensen (2008) proposes correlations for the functions given by eq.(2.4) and eq.(2.5):

$$Pr = Pr_0 + H\left(1 + \frac{3}{2}\left(\frac{\dot{m}r}{W} - 1\right) - \frac{1}{2}\left(\frac{\dot{m}r}{W} - 1\right)^3\right) \tag{2.8}$$

$$\eta = \eta_0\left(\left(1 - \left(\frac{H - H_0}{H_0}\right)^2\right) - 1000\,(\dot{m}r - 2W)^2\right) \tag{2.9}$$

Additionally, it is proposed the following relationships for the parameters *H* and *W*:

$$H = H_0 - 1.2\left(H_0 + \frac{Pr_0}{2} - 1\right) \cdot (1 - Nr) \tag{2.10}$$

$$W = W_0\,(Nr)^{\frac{1}{3}} \tag{2.11}$$

H and *W* are known as the semi-height and the semi-width, respectively, of the compressor characteristic curve. The parameters H_0 and W_0 are constant given constant values; and Pr_0 is the pressure ratio delivered when the flow is set to zero.

Finally, the compressor curves are performed by setting a constant maximum efficiency, η_0.

The fig. 2.5 shows the compressor curves presented in Jensen's work (2008) with a rotational speed in the range from 10% to 100%. The values for the different parameters are shown in table 2.1.

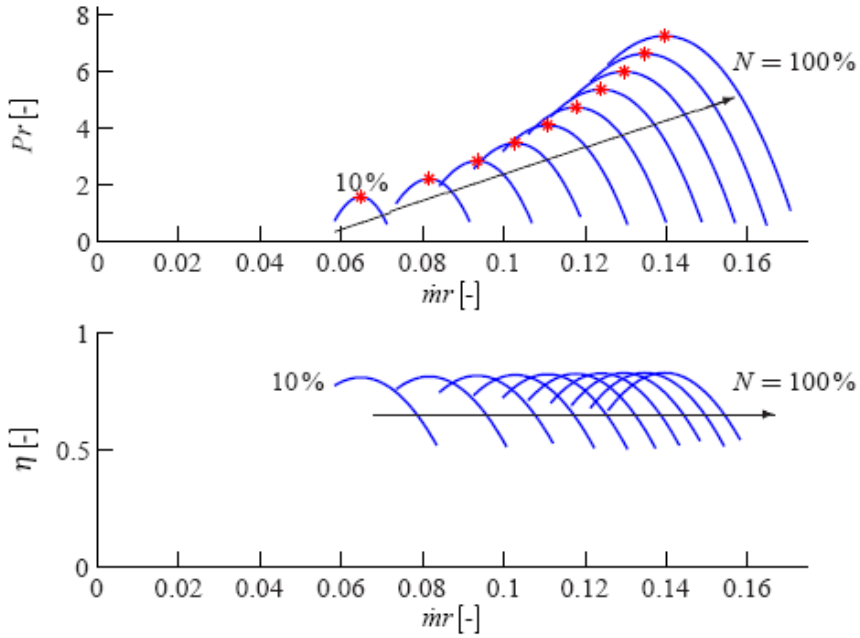

Figure 2.5. Characteristic compressor curves at nominal inlet temperature. The peak pressure ratio is indicated by the red dots.

Table 2.1. Parameter values used for the compressor curves

D	1.7 m
MW	0.032 Kg/mol
Pr_0	-29
H_0	18.125
W_0	0.0698
η_0	82.2 %

2.5 Introduction to numerical optimization

The goal of any optimization problem is to find the values of the process variables that yield the best value of the performance criterion such as minimum costs or maximum production. It is extremely helpful to systematically identify the objective, constraints, and degrees of freedom in the process (or plant) that is going to be studied.

In a typical industrial company there are three areas (levels) in which optimization is used: (1) management, (2) process design and equipment specification, and (3) plant operations. Process design and equipment specification is usually performed prior to the implementation of the process, and management decisions to implement designs are usually made far in advance of the process design step. On the other hand, optimization of operating conditions is carried out monthly, weekly, daily, hourly, or even at the extreme, every minute [5].

The solution of optimization problems involves the use of carious features of mathematics. Consequently, the formulation of an optimization problem must be carried out via mathematical expressions, although this does not necessary imply great complexity. Every optimization problem contains three essential categories:

1. At least one objective function to be optimized.
2. Equality constraints (equations).
3. Inequality constraints (inequalities).

When it is found a set of variables that satisfy categories 2 and 3, we took about a feasible solution of the optimization problem. And an optimal solution is a set of values of the variables that satisfy the components of categories 2 and 3 and also provides an optimal value for the function in category 1.

A general optimization problem can be mathematically formulated as [5]:

$$\begin{aligned} \text{Minimize (or maximize):} \quad & f(x) && \text{objective function} \\ \text{Subject to:} \quad & h(x) = 0 && \text{equality constraints} \\ & g(x) \geq 0 && \text{inequality constants} \end{aligned} \tag{2.12}$$

where x is a vector of n variables.

2.5.1 Optimization methods

The different optimization methods are related to the nature of the objective function, thus we can find two principal classifications: Unconstrained and constrained optimization problems [6].

Unconstrained optimization problems are those in which we can neglect the constraints assuming that do not have effect on the optimal solution. Also, unconstrained problems are a result of replacing the constraints by penalization terms in the objective function.

Constrained optimization problems are those models that have explicit constraints on the variables. The constraints can be linear or nonlinear inequalities. A linear programming problem is when both the objective function and the constraints are linear functions. If the objective function is nonlinear or if there is a nonlinear constraint, the optimization problem is then a nonlinear programming problem.

Many optimization methods implying complex algorithms have been developed to cover all type of optimization problems. Following, we will briefly describe two important and wide used optimization methods [7]:

- Box method, is a sequential search technique that solves problems with nonlinear objective functions, subject to nonlinear inequality constraints. It handles inequality constraints but not equality constraints. This method is not very efficient in terms of the required number of function evaluations. It generally requires a large number of iterations to converge on the solution. However, if applicable, this method is very robust.

- The Sequential Quadratic Programming (SQP) method handles inequality and equality constraints. SQP is considered by many to be the most efficient method for minimization with general linear and nonlinear constraints, provided a reasonable initial point is used and the number of primary variables are small. It minimizes a quadratic approximation of the Lagrangian function subjected to linear approximations of the constraints.

It is necessary to point out that purpose of this section is meant to only explain the basic knowledge of the work done and is not a comprehensive study on optimization methods. For further information about optimization methods, we recommend Edgar and Himmelblau (1988); and Nocedal and Wright (1999).

3 Design

This chapter will describe the work carried out on the design of the PRICO process. There will be a detailed description of the process including the employed specifications and how the process was modeled in HYSYS. Additionally, nine different cases of design are presented and the results are compared with the data reported by Jensen [4].

It is important to point out that the obtained results in this chapter do not represent the optimal design values of the process due to any optimization study was made. What is attempted is to reproduce the results found in [4] using the same design constraints. For some of the cases the results reported in [4] are used, in our model, as specifications.

3.1 Process description

In the previous chapter, it was mentioned that the PRICO process is a single mixed refrigeration cycle which uses a main heat exchanger for cooling the natural gas. The PRICO process (Fig. 3.1) mainly consists in two parts: The natural gas cooling and the refrigerant loop.

Natural gas is fed to the principal heat exchanger (NG-HX) after previous treatment removing water and impurities like carbon dioxide, hydrogen sulphide and mercury. The inlet conditions of the natural gas depend on the received pressure and temperature from the earlier treatment. In the NG-HX the natural gas is cooled, liquefied, and sub-cooled by heat exchange with the expanded refrigerant. Afterwards, the natural gas is sent to expansion where the pressure is reduced to the atmospheric and therefore the temperature is taken slightly down. In the flash drum, the liquid (LNG) is separated from the vapor phase (flash gas) which is also used as fuel. However this issue is not taken in account in this work. Finally, the LNG is sent to storage for further distribution.

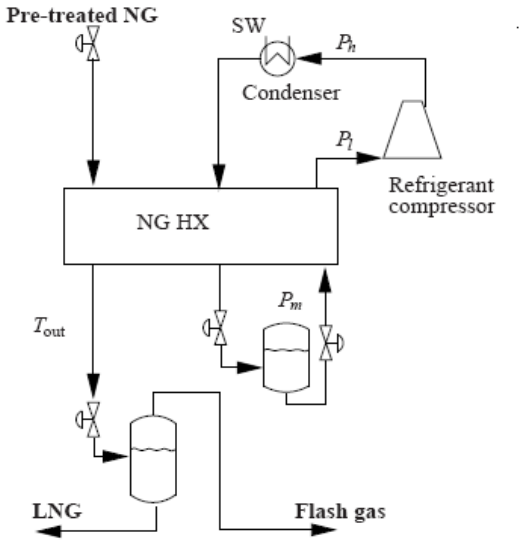

Figure 3.1. Simple flowsheet for the PRICO process

After the recompression to high pressure (P_h), the mixed refrigerant (MR) is sent to the sea water (SW) cooler where it is cooled and partially condensed. In the NG-HX, the MR is then sub-cooled at about the same temperature as the natural gas. After that, the refrigerant is expanded to low pressure (P_l) in order to reach the needed cooling temperature. Following, the refrigerant passes through the NG-HX where it is superheated by the heat gained from the two warm streams. The super heated refrigerant is then recompressed thus closing the loop.

During the study carried out the following data was used as process specifications:

- Natural gas inlet conditions: Pressure 40 bar and temperature 30 °C.
- Natural gas molar compositions[1]: 89.8% methane, 5.5% ethane, 1.8% propane, 0.1% n-butane and 2.8% nitrogen.
- The mixed refrigerant temperature after the SW cooler is 30 °C.
- There is a pressure drop of 0.1 bar in the SW cooler.
- Pressure drops in the NG-HX:
  - 5 bar on natural gas side.
  - 4 bar on the hot refrigerant side.
  - 1 bar for the cold refrigerant side.
- The suction pressure drop in the compressor is 0.3 bar.
- The components of the mixed refrigerant are: nitrogen, methane, ethane, propone and n-butane. For the nine different design cases we used the same refrigerant compositions used in [4].

3.2 HYSYS modeling

The first step of the work was to build the HYSYS model of the nominal case following the data reported in [4]. The flowsheet for the nominal case is shown in Fig. 3.2, and the specifications used are shown in table 3.1. The HYSYS model does not include the refrigerant flash drum and only one valve with the total pressure drop is used instead.

Due to how the process was modeled in HYSYS certain variables could not be change or specify directly, instead other variables were changed in order to match the desired process specifications. For this purpose an ‘adjust block’ was used. The ‘adjust’ varies the value of one stream variable (the independent variable) to meet the required value or specification (the dependent variable) in another stream or operation.

[1]It is important to note that the methane fraction is higher than the reported in Jensen’s work (89.7%) [4]. This is due to the fact that the natural gas compositions reported in [4] do not sum one, as they should be. In order to solve that misunderstanding we will use 89.8% instead

The SW cooler was modeled as a simple cooler with no heat loss and the NG-HX was modeled as an adiabatic multi-stream heat exchanger. It was considered that the two hot streams are at the same temperature after the NG-HX. That is, streams 7 and 8 are at the same temperature.

The compressor work was specified in all nine cases, while the efficiency was calculated by HYSYS. The suction pressure drop at the inlet of the compressor was modeled using an isenthalpic valve (VLV-102).

For all the calculations the SRK (Soave-Redlich-Kwong) thermodynamic fluid package was used.

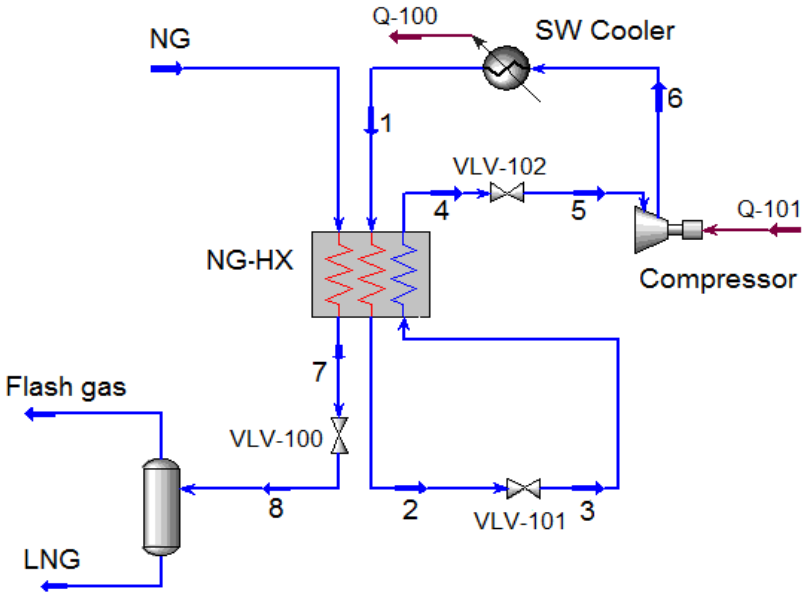

Figure 3.2. HYSYS flowsheet for designing nominal case

Table 3.1. Design constraints used to build the nominal case flowsheet

NG temperature after the NG-HX (°C)	-144
Degree of super heating, ΔT_{sup} (°C)	10
Compressor work, *Ws* (MW)	77.5
Pressure ratio, Pr	5.5
High pressure, P_h (bar)	22

3.3 Results for design

In this part of the work we will try to validate the design of the NG-HX performed earlier in Jensen's work [4]. In particular, we will compare the computed process variables for nine different cases. Each case varies the specifications of the model such as, production of flash gas ($\dot{m}_{Flash}$), compressor power (*Ws*), compression pressure (high pressure) (P_h), compressor suction volume (Vsuc) and degree of super heating (ΔT_{sup}).

The obtained results for the nine different cases are presented in Table 3.2. The numbers in parenthesis are the numbers reported by Jensen [4], and the values in boldface are the values used as active constraints or specifications. Due to the HYSYS flowsheet shown in Fig 3.2 needs a minimum set of inputs in order to be solved. For each case the optimal results are reported in [4] are used in our model as specifications.

Table 3.2. Result for the nine different cases of design

Case	3.1	3.2	3.3	3.4	3.5
$\dot{m}_{NG}$ (Kg/s)	50.69 (52.2)	**45** (45)	**45.3** (45.3)	**44.8** (44.8)	49.23 (49.6)
$\dot{m}_{LNG}$ (Kg/s)	43.27 (44.6)	41.67 (41.7)	41.97 (42)	41.47 (41.5)	45.90 (46.3)
$\dot{m}_{Flash}$ (Kg/s)	7.42 (7.7)	**3.33**	**3.33**	**3.33**	**3.33**
$\dot{m}_{Ref}$ (Kg/s)	**478** (478)	489.5 (475)	492.8 (472)	424.9 (443)	253.7 (251)
Tout (°C)	**-144**	-155.9 (-156)	**-156** (-156)	-155.8 (-156)	**-157** (-157)
ΔT_{sup} (°C)	**10**	**10**	12 (11.6)	**25.7**	**10**
Efficiency, η (%)	86.64 (82.8)	89.159 (82.8)	90.512 (82.8)	83.128 (82.8)	87.948 (82.8)
Ws (MW)	**77.5**	**77.5**	**77.5**	**77.5**	**77.5**
P_h (bar)	**22**	**22**	**22**	**22**	**50.4** (50.4)
Pr	**5.5**	**5.5**	**5.5**	**5.5**	**22.5** (22.5)
P_l (bar)	4 (4)	4 (4)	4 (4)	4 (4)	2.24 (2.24)
Vsuc (m^3/s)	90.77 (84.3)	93.07 (83.3)	94.44 (84)	86.66 (83.9)	87.1 (75.1)
UA_{HOT} (MW/°C)	31.88 (38.4)	35.33 (40.9)	35.28 (41.3)	34.21 (39.8)	14.33 (18.7)
UA_{NG} (MW/°C)	5.21 (4.8)	5.16 (4.4)	5.14 (4.4)	5.62 (4.6)	5.36 (5.7)
UA_{TOT} (MW/°C)	37.09 (43.1)	40.49 (45.3)	40.42 (45.7)	39.83 (44.4)	19.69 (24.4)

Case	3.6	3.7	3.8	3.9
$\dot{m}_{NG}$ (Kg/s)	**49.6** (49.6)	**51.4** (51.4)	**76.1** (76.1)	**80.8** (80.8)
$\dot{m}_{LNG}$ (Kg/s)	46.27 (46.3)	48.07 (48.1)	71.1 (71.1)	75.8 (75.8)
$\dot{m}_{Flash}$ (Kg/s)	**3.33**	**3.33**	**5**	**5**
$\dot{m}_{Ref}$ (Kg/s)	295.3 (298)	317.6 (320)	606.7 (611)	612.1 (617)
Tout (°C)	-157.1 (-157)	-157.5 (-157)	-157.3 (-157)	-156.4 (-156)
ΔT_{sup} (°C)	**10**	**10**	**10**	**10**
Efficiency, η (%)	82.33 (82.8)	82.31 (82.8)	82.23 (82.8)	82.47 (82.8)
Ws (MW)	**77.5**	**77.5**	**120**	**120**
P_h (bar)	**30**	**37**	**30**	**30**
Pr	14.35 (16.6)	10.73 (11.7)	6.85 (7.3)	6.77 (7.2)
P_l (bar)	2.09 (1.81)	3.447 (3.17)	4.38 (4.11)	4.43 (4.16)
Vsuc (m^3/s)	**106**	**70**	**106**	**106**
UA_{HOT} (MW/°C)	22.3 (22.9)	25.06 (26.8)	48.69 (51.8)	48.55 (52.2)
UA_{NG} (MW/°C)	7.35 (5.5)	7.33 (5.8)	10.19 (8)	10.48 (8.2)
UA_{TOT} (MW/°C)	29.65 (28.4)	32.39 (32.6)	58.88 (59.8)	59.03 (60.4)

Boldface numbers indicate specifications or active constraints
Numbers in parenthesis are the numbers reported by Jensen [4]

Case 3.1 *Nominal case*

In the HYSYS flowsheet we set the same MR flowrate (478 Kg/s) as was reported by Jensen (2008), and we let HYSYS compute the flowrate for the natural gas. The resulting natural gas flowrate was 50.69 Kg/s which was lower than the reported data by Jensen (2008) ($\dot{m}_{NG}$ = 52.2 Kg/s). However, what was important to analyze was the ratio between the LNG production and the NG fed. We found that the production ratio it was about 85.4% for both data results. Also, it is important to mention that the obtained total UA value (UA_{HOT} = 28.98 MW/°C) is lower than the one obtained by Jensen (2008) (UA_{HOT} = 28.4 MW/°C).

As we have seen, for the same process specifications we got less required heat transfer area than Jensen did (2008), but still achieved the same production ratio. This finding means that the nominal case simulated in HYSYS seems to be more efficient than the one simulated in gPROMS.

Case 3.2 *Flash gas flowrate as an active constraint*

Here the specification of T_{out} is replaced by setting the amount of flash gas as an active constraint ($\dot{m}_{Flash}$ = 3.33 Kg/s). In the HYSYS flowsheet, the MR flowrate was adjusted to match the flash gas specification. The resulting MR flow is 489.5 Kg/s (3% higher than the reported by Jensen). This increment in MR flow is offset by a reduction in the computed UA_{tot} (40.49 MW/°C), which is about 10% lower than the one reported by Jensen (2008) (45.3 MW/°C).

We should note that there is a reduction, respecting case 3.1, of the outlet NH-HX temperature (from -144 to -155.9 °C). This is due to the reduction of flash gas flowrate. The same phenomenon is found in Jensen's work.

Case 3.3 *Unconstrained degree of superheating*

In this case we specified the same value for the natural gas feed-rate as in Jensen's work (2008) ($\dot{m}_{NG}$ = 45.3 Kg/s) and as result we got the same outlet NG-HX temperature, T_{out} = - 156 °C.

By leaving free the degree of superheating specification (ΔT_{sup}), it is computed by the HYSYS flowsheet. The obtained degree of superheating increases from 10 to 12°C compared with case 3.2. This increment in ΔT_{sup} increases the LNG production in about 0.7%, which is pretty similar to the one reported by Jensen (2008) (0.8%). This increment in the LNG production shows to the fact that for a system with internal heat exchange the optimal ΔT_{sup} is not zero (Jensen and Skogestad, 2007).

Case 3.4 *Higher degree of superheating*

For this case, first we specified the desired degree of superheating (ΔT_{sup} = 25.7 °C) and we let HYSYS calculate the T_{out}.

In order to match the flash gas specification, we adjusted the MR flowrate. The obtained MR flow (424.9 Kg/s) is about 13.8% lower than reported for case 3.3 (492.8 Kg/s), and the UA_{tot} decreases about 1.5%. Even though these reductions in the MR flow and in the heat transfer area, the LNG production is only reduced to 1.2%. This reaffirms what it is stated by Jensen, that 'the optimum is flat in terms of superheating'. For the same case, Jensen reports a reduction of 1.3% in LNG production.

Case 3.5 *No pressure constraints*

In this case we set the same pressure ratio and high pressure that were found by Jensen (2008) (Pr = 22.5 and P_l = 2.24 bar). Additionally, T_{out} is set to -157°C and the MR flowrate is adjusted to match the flash gas specification. We found that there was an increment in the LNG production of 9.2% respective to case 3.2 (LNG production increases from 41.67 to 45.90 Kg/s). It is also important to note that both the refrigerant flowrate and the total heat transfer area decrease about 48% and 51% respectively.

As we saw, a high pressure ratio leads to increase the LNG production. This is also found and explained by Jensen (2008): The cooling duty per Kg of refrigerant is directly linked to compressor head. As the compressor head increases the cooling duty per Kg of refrigerant increases, and as it is known by increasing the pressure ratio, the compressor head is also increased. Therefore, an increment in the pressure ratio indicates that an increment in the cooling duty per Kg of refrigerant, and consequently less UA_{tot} is needed. The needed refrigerant flow is also reduced by this fact.

Even though high pressure ratio designs increase the LNG production, these types of designs are not common due to more compressor stages (casings) that are needed.

Case 3.6 *MCL1800 series compressor*

In this case, we work with a centrifugal compressor MCL1800. The following compressor data is given [4]:

- Diameter: 1800 mm
- Maximum suction volume: 106 m^3/s
- Maximum outlet pressure: 30 bar
- Maximum work: 120 MW

For this case the suction volume and the outlet pressure are set to their maximums, while the compressor work is kept in 77.5 MW.

In the HSYSYS flowsheet the MR flowrate was again adjusted to match the specified flash gas flowrate (3.33 Kg/s), and the compressor inlet pressure (P_l) was adjusted to match the suction volume of 106 m^3/s.

We found that the LNG production is 46.27 Kg/s, which is 0.8% higher than the one for case 3.5. This result is important since we are working with realistic specifications and not with impractical designs like in case 3.5. This fact is also shown and discussed by Jensen (2008).

Case 3.7 *MCL1400 series compressor*

The following data is given for the MCL1400 series compressor:

- Diameter: 1400 mm
- Maximum suction volume: 70 m^3/s
- Maximum outlet pressure: 37 bar
- Maximum work: 75 MW

Here we use the maximum suction volume and the maximum discharge pressure. The work is assumed to be 77.5 MW as the previous cases.

In order to match the specifications of flash gas and volume suction, the same method describe in case 3.6 was used.

As in Jensen's work, there is an increment in the LNG production (about 3.7%) respect case 3.6, $\dot{m}_{LNG}$ increases from 46.27 to 48.07 Kg/s.

Case 3.8 *MCL1800 series compressor at maximum power*

As we did in Case 3.6, we needed to adjust the MR flowrate to match the specified flash gas flowrate (3.33 Kg/s), and to adjust the compressor inlet pressure (P_1) to match de suction volume of 106 m^3/s. We also set the natural gas feed rate and let HYSYS to calculate T_{out}, resulting in T_{out} equal to -157.3 °C.

Since an isentropic expansion process provides more cooling than an isenthalpic process, the isenthalpic valve could be totally replaced for a isentropic liquid turbine. In theory, the efficiency of the refrigeration system is improved by applying this change. However, liquids tend to become vapor during the expansion step, which can affect the safety of the turbine.

In order to avoid vapor formation in the liquid turbine, a combination of a liquid turbine and a valve must be employed. Thus, the expansion process is broken down into two steps: First the turbine reduces the pressure (the resulting pressure slightly above the saturation pressure) and then the two phase expansion is made in the isenthalpic valve.

In the figure below (fig 3.3), a simple flowsheet is shown of the PRICO process which uses liquid turbines for the expansion of the natural gas and the refrigerant.

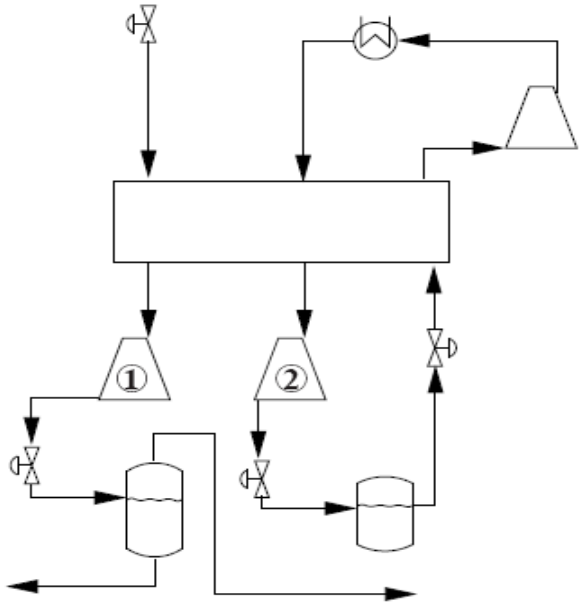

Figure 3.3. Simple flowsheet of the PRICO process using liquid turbines for the expansion of the natural and the refrigerant

Case 3.9 *Liquid turbines for the expansion of the natural gas and refrigerant*

There is a LNG production increment of 6.6% with respect to case 3.8 (same increment reported by Jensen). Additionally, we found an increment of 0.25% in the total heat transfer area compared to case 3.8. The UA_{TOT} increment reported by Jensen is 1%.

This design, as was expected, gives the maximum LNG production. A design using only a liquid turbine could be used; however, we already know that in practice this will not be possible.

It is important to note that in Jensen's work (2008), the compressor efficiency is set as a constant with a maximum value of 82.8%. However, the results in Table 3.2 show that we got higher compressor efficiencies for cases 3.1, 3.2, 3.4 and 3.5. The reason for the higher efficiencies in our model is because the compressor efficiency cannot be set. In order to be solve the compressor model in HYSYS it needs:

- the inlet and outlet pressures, and other specification like compressor power/efficiency, or

- the compressor power, compressor efficiency and one of the working pressures.

In the HYSYS flowsheet, shown in Fig. 3.2, the pressure of streams 4 and 6 are set according to the high pressure, low pressure and pressure ratio specifications. Furthermore, only one more specification can be specified. As the compressor power has to be specified for all cases, the efficiency is then computed by the flowsheet.

3.4 Conclusions

The main goal of this chapter was to reproduce the design results reported by Jensen (2008). We saw throughout the work that all the design variables were matched properly, so we can conclude the following:

- The nominal case (3.1) simulated in HYSYS seems to be more efficient than the one reported by Jensen (2008). Therefore, we got a higher LNG production for a lower UA_{TOT}.

- The degree of superheating increased when it was unconstrained, which produced an increment in the LNG production. This showed the fact that for a system with internal heat exchange, the optimal ΔT_{sup} is not zero (this extensively discussed by Jensen and Skogestad, 2007).

- The LNG production is only reduced to 1.2% compared to 3.3, by setting a higher degree of super heating. This reaffirms what is stated by Jensen, that 'the optimum is flat in terms of superheating' [4]. For the same case, Jensen reports a reduction of 1.3% in LNG production.

- Even though high pressure ratio designs increase the LNG production, these types of designs are not common due to more compressor stages (casings) that are needed.

3.5 Further work

In order to be sure that the obtained results are the optimum values, it is necessary to carry out an optimization study. Jensen (2008) provides the objective function for the optimization problem. The objective function proposed in Jensen's work is:

$$f = - \dot{m}_{LNG} + C_0 \cdot (A_{HOT}^{0.65} + A_{NG}^{0.65}) \quad (3.1)$$

Then the optimization problem for design can be solved by minimizing f with respect to the design parameters A_{HOT} and A_{NG} and adjusting C_0 to get the logical values for the minimum temperature approach.

An interesting task would be to find (using HYSYS) the optimal design variables for the nine studied cases, and compare and see if these values match with the results presented in this paper and in Jensen's work.

4 Optimal operation

The simulation of LNG processes is crucial because it is the only cost-effective method by which design improvements can be tested. Proposed LNG plants are simulated, designed, and then built full-scale. The optimal design of mixed refrigerant systems is extremely difficult and a lot of work is pointed in that direction. Even though an optimal design does not necessary imply an optimal operation of the process, few works are focused in the optimal operation study.

In this part of the work we will seek the optimal steady state operating conditions for the PRICO process, in two different modes:

- **Mode I:** In this case the production of LNG is a specification and we try to minimize the compressor work.

- **Mode II:** In this case the compressor work is set and the goal is to maximize the LNG production.

After finding the optimal conditions for both modes, some disturbances are introduced to the system. The process will be re-optimized and we will study the effect of each disturbance over the system. These disturbances will be: compressor work, feed pressure, natural gas and mixed refrigerant temperatures, natural gas feed rate.

Finally, we will compare the obtained results with the ones reported by Jensen [4].

4.1 Process description

The PRICO process employed in this part of the work (Fig. 4.1) is a modification of the nominal case studied in the chapter before. Specifically, we will work with the ninth case where two liquid turbines are added to expand the natural gas and then mixes refrigerant after being cooled in the main heat exchanger. The modified process works similarly as the nominal case:

- Natural gas is fed to the NG-HX where it is cooled, liquefied and sub-cooled. After that, it is sent to a liquid turbine to be expanded and therefore its temperature gets lower. The following isenthalpic valve gives the necessary pressure drop to reach the necessary outlet pressure (atmospheric pressure). Finally, the liquid (LNG) and the vapor phase (Flash gas) are separated in a flash drum.

- The mixed refrigerant is compressed to high pressure (P_h) and afterwards it is cooled down in the sea water (SW) cooler. Then, the refrigerant is sub-cooled in the NG-HX along with the natural gas stream. The resultant sub-cooled refrigerant is then expanded to low pressure (P_l), first in a liquid turbine and secondly by a choke valve. The given pressure drop produces a two phase mixture which is vaporized and slightly superheated in the NG-HX, thus providing the necessary cooling duty.

As a final step, the refrigerant loop is closed with the refrigerant recompression from P_l to P_h. The PRICO process discussed above is shown in Fig. 4.1.

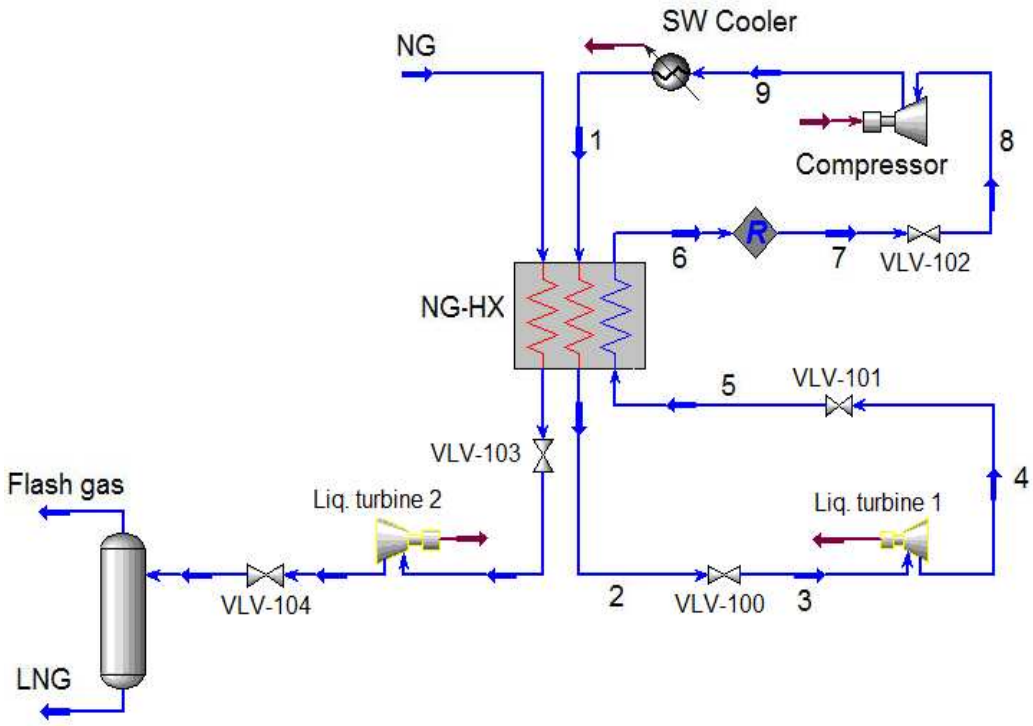

Figure 4.1. HYSYS flowsheet for PRICO process used for optimal operation

4.1.1 Nominal conditions

For the nominal operation of the process, the following data was used:

- Natural gas inlet conditions: Pressure 40 bar and temperature 30 °C.
- Natural gas feed rate = 74.33 Kg/s.
- The natural gas temperature after the NH-HX is -157 °C.
- The mixed refrigerant temperature after the SW cooler is 30 °C.
- There is a pressure drop of 0.1 bar in the SW cooler.
- Pressure drops in the NG-HX:
  - 5 bar on natural gas side.
  - 4 bar on the hot refrigerant side.
  - 1 bar for the cold refrigerant side.

- The suction pressure drop in the compressor and turbines is 0.3 bar.
- The pressure drop in VLV-104 is 3.15 bar.
- The maximum compressor work is 120 MW.
- The heat transfer coefficients (UA) are considered constants.
- Natural gas molar compositions[2]: 89.8% methane, 5.5% ethane, 1.8% propane, 0.1% n-butane and 2.8% nitrogen.
- The used refrigerant compositions are the reported by Jensen [4].

4.1.2 Degrees of freedom

In the PRICO process, shown in Fig. 4.1, there are 9 variables that can be manipulated:

- Compressor speed
- Valve opening (VLV-101)
- Turbine power (Liq. Turbine 1)
- SW flowrate
- NG feed rate
- Mixed refrigerant composition (4 independent compositions)

One degree of freedom is consumed by specifying the temperature after the SW cooler (T_1 = 30 °C). So, there are 8 remaining degrees of freedom that can be used to find the nominal optimal conditions. For this work we will not do any optimization or study involving the mixed refrigerant composition, instead we will use for all cases the same refrigerant composition reported by Jensen (2008). So, the mixed refrigerant compositions are considered constant and that consumes 4 degrees of freedom.

So, in principle there are 4 degrees of freedom left to be used to find the nominal optimum steady state operating conditions. It is important to note that since the refrigerant composition is assumed to be constant for all cases then the degrees of freedom for optimization are the same for operation.

[2] The issue about the difference between the methane fraction used and the one reported in Jenses's work [4] was already discussed in section 3.1.

4.2 HYSYS modeling

Due to the equipment data being fixed during operation; it is indispensable to modify some elements of the model when we switch from design to operation mode. As it was seen in the chapter before, when we studied nine different design cases of the PRICO process, the UA values were always results computed by the HYSYS flowsheet. However, during the operation mode, the UA values must be set as specifications of the model. Another important issue that has to be taken into account is the compressor behavior. In operation mode the performance of the compressor is modeled using characteristic curves that relate flow, efficiency, pressure ratio and rotational speed.

The SW cooler was again modeled as a simple cooler with no heat loss and the NG-HX was modeled as an adiabatic multi-stream heat exchanger.

The suction pressure drops for the compressor and the turbines were modeled using isenthalpic valves before each one (VLV-100, VLV-102, VLV-103).

For all the calculations in the model the SRK (Soave-Redlich-Kwong) thermodynamic fluid package was used.

A 'recycle block', which uses the MR flowrate and T_7 as initial guesses, was also included in the flowsheet. This is due to the refrigerant flow is needed to solve the NG-HX and T_7 is needed to run the compressor. But, since no one of these variables are known it is necessary to use the 'recycle block'. First, HYSYS uses the conditions of the stream 7 and solves the flowsheet up to the stream 6. HYSYS then compares the values of the stream 6 to those in the stream 7. Based on the difference between the values, HYSYS modifies the values in the stream 6 and passes the modified values to the stream 7. The calculation process repeats until the values in the stream 6 match those in the stream 7 within specified tolerances.

4.2.1 Compressor model

As we saw in Chapter 2, during operation it is usual to model the behavior the compressor by characteristic curves that link the different compressor variables. The compressor curves presented in Chapter 2 (Fig. 2.5) express the pressure ratio and the compressor efficiency in terms of rotational speed and reduced mass flow.

HYSYS allows setting the characteristic curves for a compressor in terms of volumetric flow, compressor head and efficiency for a given speed. Therefore, the used curves were not exactly the same as those shown in fig 2.5. The curves we used (Fig. 4.2) are varieties which correlate the head, flowrate and efficiency of the compressor with compressor speed in the range from 300 to 1200 rpm. HYSYS uses these characteristic curves to calculate the stream outlet conditions and the compressor variables for a certain flowrate.

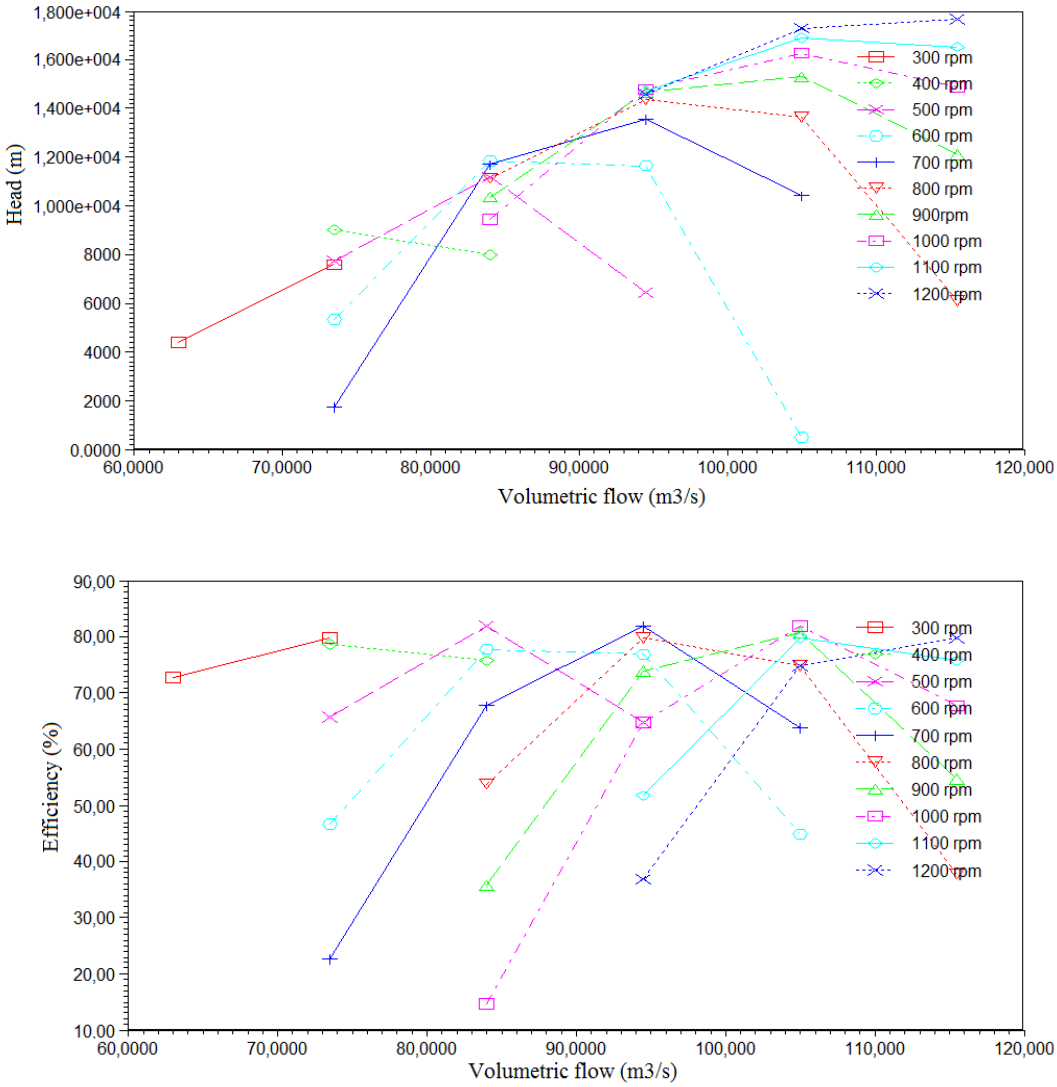

Figure 4.2. Compressor curves for HYSYS model

4.3 Solving optimization problem

In Chapter 2 we saw that any optimization problem must be done using mathematical expressions; although this does not necessary imply great complexity. In a normal design optimization, the capital and operational costs have to be included into the optimization problem. For optimal operation it is assumed that all the equipment investment has been done, thus only the operational costs are taken into account in the optimization problem.

The objective function for optimal operation is taken from [4] and it represents the annual operating costs ($/year):

$$f = Pw_s \cdot W_s - Pw_t \cdot W_t + Psw \cdot Qc - P_{LNG} \cdot \dot{m}_{LNG} + P_{NG} \cdot \dot{m}_{NG} - P_{Flash} \cdot \dot{m}_{Flash} \qquad (4.1)$$

In order to simplify the objective function, some assumptions have to be done:

- We consider the same price for natural gas and flash gas, $P_{NG} = P_{Flash}$. This assumption is understandable because the natural gas and the flash gas can both be used as fuel gases.

- The profit generated by the turbines is neglected, $Pw_t = 0$. The advantage of using liquid turbines is the extra cooling, not the generated power.

- The cost of cooling in the SW cooler is neglected, $Psw = 0$. Since we are using sea water for cooling, this only needs to be pump to the plant. The power consumption used to pump the water is much lower than the used for the compressor.

Additionally, the following material balance has to be taken in account: $\dot{m}_{NG} = \dot{m}_{LNG} + \dot{m}_{Flash}$

Finally, the resulting objective function is:

$$f = Ws - \hat{P}_{LNG} \cdot \dot{m}_{LNG} \qquad (4.2)$$

As f represents the annual operation costs, it should be minimized in order to get the maximum possible profit. Therefore, the optimal conditions of the process are found by minimizing eq. (4.2) subject to the different constraints. The process optimization is carried out in two different operational modes:

- **Mode I:** In this mode the natural gas feed rate (or LNG production) is specified. Then the optimization problem results:

$$\begin{aligned} & \min f \rightarrow \min Ws \\ \text{subject to:} \quad & \dot{m}_{NG} = \text{given} \quad (\text{or } \dot{m}_{LNG} = \text{given}) \\ & c \geq 0 \end{aligned} \qquad (4.3)$$

- **Mode II:** With a given compressor work, and considering high LNG price ($\hat{P}_{LNG}$) the optimization problem turns in:

$$\begin{aligned} & \min f \rightarrow \max \dot{m}_{LNG} \\ \text{subject to:} \quad & Ws = Ws^{max} \\ & c \geq 0 \end{aligned} \tag{4.4}$$

For both modes, $c \geq 0$ represents the inequality constraints that should be satisfied to guarantee a feasible solution.

4.3.1 Optimization in HYSYS

Once the flowsheet converged, we employed the HYSYS steady state optimizer to find the operating conditions that solved optimization problem given by equations 4.3 and 4.4. The optimizer has its own spreadsheet where we can define the objective function and the constraint expressions. In order to run the optimization, the optimizer needs then following information [7]:

- Objective function
- Primary Variables. Variables whose values are manipulated in order to minimize (or maximize) the objective function.
- Constraints. The inequality and equality constraint functions can be also defined in the optimizer spreadsheet.

It is really important to set appropriate upper and lower variable bounds to prevent bad flowsheet conditions (e.g., temperature crossovers in Heat Exchangers).

The optimizer is a powerful tool that allows choosing between different optimization methods [7]:

- The box, mixed and the Sequential Quadratic Programming (SQP) methods are available for constrained optimizations with inequality constraints.
- The Original and Hyprotech SQP methods can handle equality constraints.
- The Fletcher-Reeves and Quasi-Newton methods are available for unconstrained optimization problems.

The chosen optimization method was the mixed method, which requires the least number of function evaluations (it is the most efficient). The mixed method takes advantage from the box method and the SQP method. It starts the optimization with the box method using a very loose convergence tolerance. After convergence, the SQP method is used to locate the final solution using the desired tolerance.

4.4 Nominal optimum

4.4.1 UA values for optimization

As we have said before, during the optimization mode the UA values for the NG-HX have to be set in the HYSYS flowsheet. These UA values must supply the necessary heat transferred per unit area to guarantee that all the temperature specifications related to the NG-HX are matched.

As starting point we tried to use the same UA values reported by Jensen [4], but the temperature specifications could not be matched. This means that using those UA values the outlet temperature of the natural gas was higher than -157 °C, therefore we had to find out new UA values.

In order to get the new UA values, we specified as many temperatures as necessary for the NG-HX to solve. Trying to get the same results we used the same temperatures and flows reported in Jensen's work [4]. Specifically, the outlet temperature of the warm refrigerant and natural gas were both set to -157 °C, and we let HYSYS to calculate the UA values. Even though we used the same data as in Jensen's work [4], different UA values were found. The table 4.1 shows the new UA values:

Table 4.1. UA values used in optimization

UA for natural gas in NG-HX, UA_{NG}	11.86 MW/°C
UA for warm refrigerant in NG-HX, UA_{HOT}	51.70 MW/°C
UA for cold refrigerant in NG-HX, UA_{TOT}	63.56 MW/°C

The total UA value that we got is higher than the one reported by Jensen (61.6 MW/°C) [4]. That difference could be due to the way of how HYSYS solve the flowsheet. In any case, what it is important to remark is that the difference between the obtained and the expected total UA value is not that big (about 3.2 %). For the further optimization studies we will use the new UA values.

4.4.2 Mode I: Nominal optimum for given production

In this case, the natural gas feed rate is the value reported in section 4.1.1 (74.33 Kg/s) and the optimal operation conditions are found by solving the optimization problem in Eq. 4.3. The results are presented in table 4.2.

The optimization problem demands us to identify the optimization variables and the possible inequality constraints.

We already saw that there are remaining 4 degrees freedoms because 4 degrees of freedom are consumed by specifying the MR composition and the other degree of freedom is consumed by setting the temperature equal to 30 °C at the outlet of the SW cooler. Since the NG feed rate is specified another degree of freedom is consumed. One of the three remaining degrees of freedom is consumed by setting the compressor speed. Another degree of freedom is consumed by specifying T_{out} = -157 °C. Thus, only on degree of freedom left, the low pressure (P_l).

It is important to note that the MR flow rate is not a real specification since it is determined in the 'stream 7' at the outlet of the 'adjust block'. The MR flow rate is used by the 'adjust' as a starting point to solve the flowsheet. Therefore, the 'adjust' will calculate the final flowrate which then matches all the process constraints.
So, the nominal optimum was solved respect to two optimization variables: low pressure and MR flow rate.

According to our model, the pressure drop in VLV-101 was computed by HYSYS. During the optimizations, this valve is used to register negative pressure drop. This negative pressure drop occurs because the refrigerant temperature at the inlet of the NG-HX (T_5) should be as low as possible in order to cool the natural gas and the hot refrigerant. When T_5 is not low enough, the system tries to assign an extra pressure drop to the liquid turbine. This extra pressure drop is only supported by a negative pressure drop in the valve because increasing the pressure through the valve allows the turbine to have a bigger pressure drop. Therefore, the necessary cooling temperature is reached by the extra cooling given by the turbine.

In order to avoid this behavior, we set an inequality constraint for the pressure drop of VLV-101. Thus, the optimization problem given by Eq. 4.3, is subject to:

$$\Delta P_{VLV\text{-}101} \geq 0.$$

After running the optimization case with the already mentioned variables and constraints, we found the operating optimal conditions for Mode I. The results are summarized in Table 4.2.

Table 4.2. Optimal conditions for operation: Mode I and mode II.

	Mode I	Mode II	Mode II*
MR flowrate, $\dot{m}_{Ref}$ (Kg/s)	543.7 (549)	613.1 (614)	612.4
LNG flowrate, $\dot{m}_{LNG}$ (Kg/s)	**69.99**	77.88 (76.7)	77.88
High pressure, P_h (bar)	26.64 (26.8)	29.51(30)	30.98
Low pressure, P_l (bar)	3.998 (3.67)	4.5 (4.14)	4.25
NG temperature after cooling, Tout (°C)	**-157**	**-157**	**-157**
Compressor speed, N (rpm)	**1000**	**1000**	**1000**
Compressor efficiency, η (%)	81.88 (82.8)	81.73 (82.8)	82.7
Compressor work, *Ws* (MW)	106 (106)	**120**	**120**

Boldface numbers indicate specifications or active constraints
Numbers in parenthesis are the numbers reported by Jensen [4]
*Optimized Mode II using refrigerant composition of Mode I

The optimization study carried out gave an optimal compressor work of 106 MW, and as we can see in Table 4.2 the obtained result matches perfectly to the one reported by Jensen. Additionally, the optimal compressor ratio (Pr = 6.66) is about 8.8% lower than the one found by Jensen (2008) (Pr = 7,3).

Since we used the same feed rate (74.33 Kg/s) and the same T_{out} (we specified T_{out} = -157 °C) reported in [4] we should get the same LNG production. However, the LNG production reported in [4] ($\dot{m}_{LNG}$ = 69.8 Kg/s) is slightly lower to the one we obtained ($\dot{m}_{LNG}$ = 69.99 Kg/s). This difference could be due to not using the exact- same natural gas composition as the one used in Jensen's work [4].

4.4.3 Mode II: Nominal optimum for given power

In this mode, the compressor work was set to its maximum value (120 MW) and, as we saw in section 4.3, the optimal operation is found by solving Eq. 4.4.

Here it is valid the same degrees of freedom analysis carried out in previous section: First we start with 4 degrees of freedom and one of them is consumed by specifying the compressor rotational speed. Another degree of freedom is consumed by setting T_{out} = -157 °C. And the last one is consumed to match the specified compressor work. So, as in the previous case, the nominal optimum is found by using the optimization variables: low pressure and MR flow rate.

In order to find the nominal optimum, we had to make some changes to the original flowsheet. First, the compressor work could not be directly specified because the compressor curves were entered into the HYSYS flowsheet. Instead, we had to used an 'adjust block' which adjusted the refrigerant flow ($\dot{m}_7$ in Fig. 4.1) to match the given compressor work.

The optimization problem for this mode, as found in mode I, is also subject to the constraint: $\Delta P_{VLV\text{-}101} \geq 0$. In order to satisfy this constraint, the low pressure (P_6 in Fig 4.1) was adjusted by using an 'adjust block'.

Finally, the optimization problem was solved by increasing the natural gas feed rate until no feasible solution was found. The obtained results are summarized in Table 4.2.

In Table 4.2 we can see that the obtained LNG production is 1.5% higher than the one reported by Jensen. This means we computed better nominal conditions then Jensen for the given compressor work.

4.4.4 Nominal optimum refrigerant composition

We have mentioned before that the same refrigerant composition reported in [4] was used for each case. In other words, we did not do any optimization concerning the refrigeration composition.

Jensen reports different refrigerant compositions for the nominal optimum in Mode I and Mode II. The reported refrigerant compositions are supposed to be the optimal values for each case. However, we did the optimization of Mode II using the same refrigerant composition reported for Mode I. For these conditions we got very similar results (see Table 4.2). Surprisingly, we managed to obtain the same LNG production ($\dot{m}_{LNG}$ = 77.88 Kg/s) by the given compressor work of 120 MW. It was interesting that we could achieve all the Mode II specification and constraints using the refrigerant composition of Mode I.

In Jensen's work the refrigerant composition was treated as a disturbance. The refrigerant fractions of methane (C_1), ethane (C_2), butane (C_4) and nitrogen (N_2) were changed and then were introduced into the system as disturbances. Looking at Jensen's work we find that for Mode II, the LNG production first increases and then decreases as a function of the refrigerant methane fraction (from 28.7 to 35.1%). And the same trend is founded for the other refrigerant components. This behavior in the LNG production could explain why we got in Mode II the same LNG production for two different sets of refrigerant composition. That is, while the increment of some component causes the reduction of the LNG production, the reduction of other component leads to an increase in the LNG production. Thus, the LNG production is stabilized at its optimal value.

4.5 Optimal operation with disturbances

Since the rotational speed is not a specification there is one degree of freedom more. Therefore the optimization variables are: The rotational compressor speed, the low pressure and the MR flow rate. Remember that the MR flow rate is not a real specification of the process. It is just used by the 'adjust' like a starting guess.

4.5.1 Mode I

- **Natural gas feederate**

In table 4.3, we can see the optimal values for the process variables for when the natural gas flowrate is introduced as a disturbance. As we can expect, the compressor work increases by increasing the amount of natural gas that has to be liquefied.

Also, we can note that at $\dot{m}_{NG}$ = 70.61 Kg/s, the flash gas flowrate is 4.12 Kg/s, and for $\dot{m}_{NG}$ = 70.61 Kg/s it is 4.44 Kg/s (7.2% of increment). So, even though we can increase the NG feed rate, more NG is going to behave like flash gas (which is undesired) and not as LNG. In other words, it is not always optimal to simply increase the amount of NG fed; we have to take care of other issues in this case.

Table 4.3. Mode I optimal conditions with NG flowrate as disturbance

	NG flow = 70.61 Kg/s	NG flow = 72.47 Kg/s	NG flow = 74.33 Kg/s	NG flow = 76.19 Kg/s	NG flow = 78.05 Kg/s
$\dot{m}_{Ref}$ (Kg/s)	537.7	532.5	543.7	565.9	-
$\dot{m}_{LNG}$ (Kg/s)	66.49	68.24	69.99	71.75	-
P_h (bar)	24.87	25.74	26.64	27.36	-
P_l (bar)	4	3.951	3.998	4.097	-
N (rpm)	941.4	990.5	1000	973.1	-
η (%)	81.029	81.91	81.884	81.668	-
Ws (MW)	102.713	103.417	106.003	109.361	-

In the Fig 4.3, it is represented the compressor work as a function of the LNG flowrate. We can see that the obtained trend is equivalent to the one presented in Jensen's work (2008). Actually, we observe that our curve is always beneath the curve reported by Jensen. This means we obtained more optimal conditions (less compressor work for the same LNG production).

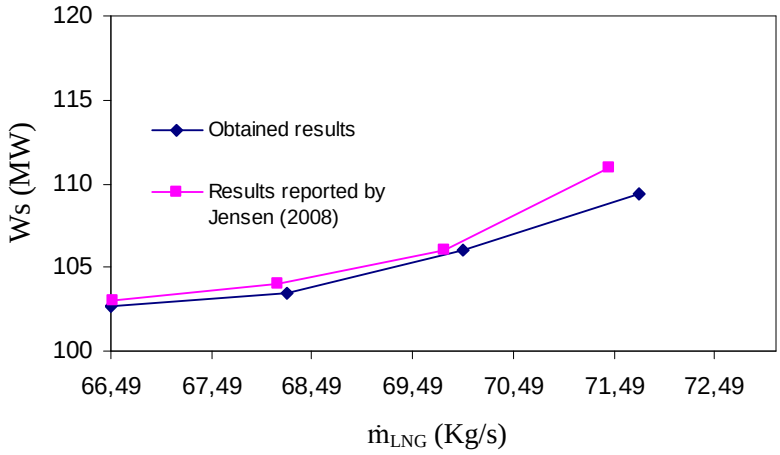

Figure 4.3. Mode I compressor work as a function of LNG flowrate

- **Natural gas feed temperature (T_{NG})**

In the Table 4.4 and in the Fig.4.4 we can see that the compressor work slightly increases as increasing the NG temperature. It is easy to see that the values for the process variables are not too different between one another. Specifically, the compressor work only increases by 0.5%, from T_{NG} =25°C to T_{NG} =35°C. This fact suggests that the optimum process variables are "flat" in terms of NG temperature.

Table 4.4. Mode I optimal conditions with NG temperature as disturbance

	T_{NG}= 25 °C	T_{NG} = 27.5 °C	T_{NG} = 30 °C	T_{NG} = 32.5 °C	T_{NG} = 35 °C
$\dot{m}_{Ref}$ (Kg/s)	545.2	545.7	543.7	544.1	544.1
P_h (bar)	26.49	26.51	26.64	26.64	26.65
P_l (bar)	4	4	3.998	4	4
N (rpm)	987.6	987.3	1000	998.8	999.8
η (%)	81.807	81.906	81.884	81.951	81.994
Ws (MW)	105.745	105.905	106.003	106.132	106.273

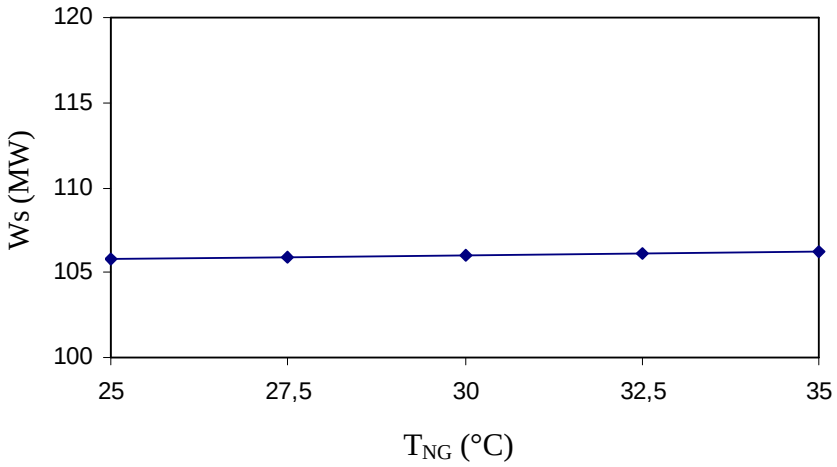

Figure 4.4. Mode I compressor work as a function of NG temperature

- **Natural gas feed pressure (P_{NG})**

As we can observe in Table 4.5, the needed refrigerant decreases by increasing the fed pressure of the natural gas. Consequently, the compressor needs less power to compress the refrigerant flow from P_h to P_l. The compressor work registers a reduction of about 6.5% for all the range of study (from 35 to 45 bar). This change in compressor work is much higher than the one calculated by NG temperature as disturbance (only 0.5%), so we can state that the system is strongly affected by the natural gas feed pressure. The effect of the NG pressure over the compressor is shown in Fig 4.5.

Table 4.5. Mode I optimal conditions with NG pressure as disturbance

	P_{NG} = 35 bar	P_{NG} = 37.5 bar	P_{NG} = 40 bar	P_{NG} = 42.5 bar	P_{NG} = 45 bar
$\dot{m}_{Ref}$ (Kg/s)	563	571	543.7	541	532.3
P_h (bar)	28.23	27.17	26.64	25.81	25.36
P_l (bar)	4.057	4.115	3.998	4.002	4
N (rpm)	996.3	953.7	1000	974.6	971.3
η (%)	81.535	81.389	81.884	81.72	81.34
Ws (MW)	110.332	109.388	106.003	104.646	103.181

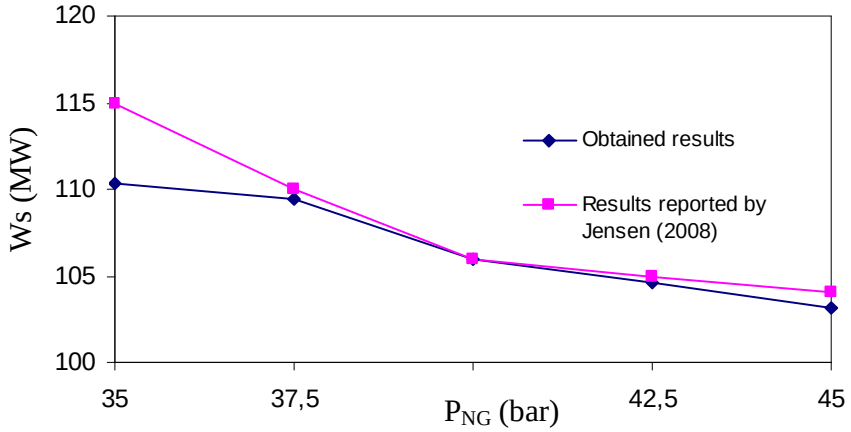

Figure 4.5. Mode I compressor work as a function of NG pressure

In the Fig. 4.5 shown above, we can see the performance of the compressor work as a function of natural pressure. Note that the curve presented by Jensen (2008) follows the same trend as our data. Also, Jensen's curve seems to be more affected by the natural pressure (it presents a work reduction of about 9.6%). However, the obtained curve in this paper, presents lower compressor work for the entire pressure range under study. It means that for this case we have got more optimal results.

- **Mixed refrigerant temperature after the SW cooler (T_7)**

The temperature of the available cooling water can easily change with the weather conditions, so it is important to analyze how the temperature of the SW cooler affects the system. In table 4.6, the optimal conditions for T_7 acting as disturbance are presented. We can note that the compressor work increases by increasing T_7 and the total increment in the compressor work is about 3.8%. No feasible solution was found for T_7 = 33 °C, this is acceptable because a high cooling temperature is never desired.

Table 4.6: Mode I optimal conditions with MR temperature as disturbance

	T_7 = 27 °C	T_7 = 28.5 °C	T_7 = 30 °C	T_7 = 31.5 °C	T_7 = 33 °C
$\dot{m}_{Ref}$ (Kg/s)	560.5	550.6	543.7	563.6	-
P_h (bar)	25.71	26.05	26.64	26.92	-
P_l (bar)	4.01	3.985	3.998	4.148	-
N (rpm)	906.8	951.3	1000	972.5	-
η (%)	80.992	81.436	81.884	81.613	-
Ws (MW)	104.723	105.351	106.003	108.852	-

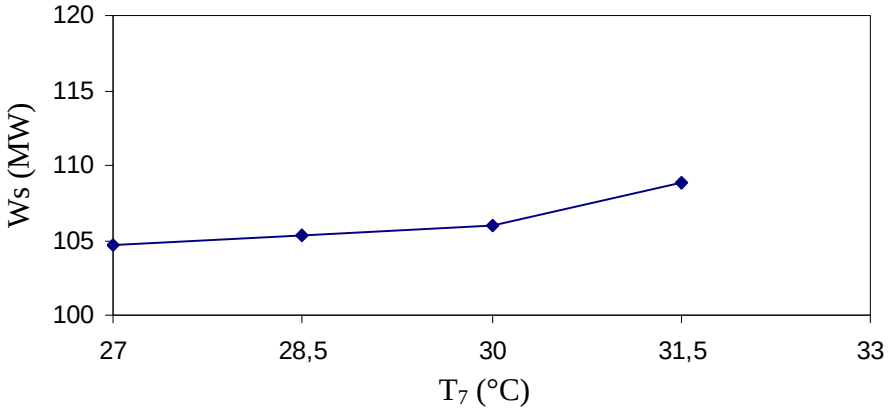

Figure 4.6. Mode I compressor work as a function of MR temperature

- **Temperature of natural gas and mixed refrigerant at the inlet of the main heat exchanger (T_{in})**

In this case, we consider both the natural gas and refrigerant temperatures as disturbances. For this case the compressor work increase (as it is expected) 15% from T_{in} = 25 °C to T_{in} = 35 °C. The obtained compressor work change is the highest for the operation in Mode I. Therefore, this disturbance is the one which affects the process the most. The optimal results for this case are presented in the Table 4.7:

Table 4.7. Mode I optimal conditions with NG and MR temperature as disturbances

	T_{in} = 25 °C	T_{in} = 27.5 °C	T_{in} = 30 °C	T_{in} = 32.5 °C	T_{in} = 35 °C
$\dot{m}_{Ref}$ (Kg/s)	548	554.2	543.7	573.4	603.4
P_h (bar)	25.22	25.65	26.64	27.36	29.49
P_l (bar)	3.875	3.965	3.998	4.23	4.5
N (rpm)	902	925.5	1000	973.8	1000
η (%)	80.838	81.219	81.884	81.641	79.281
Ws (MW)	102.127	104.634	106.003	110.811	120.069

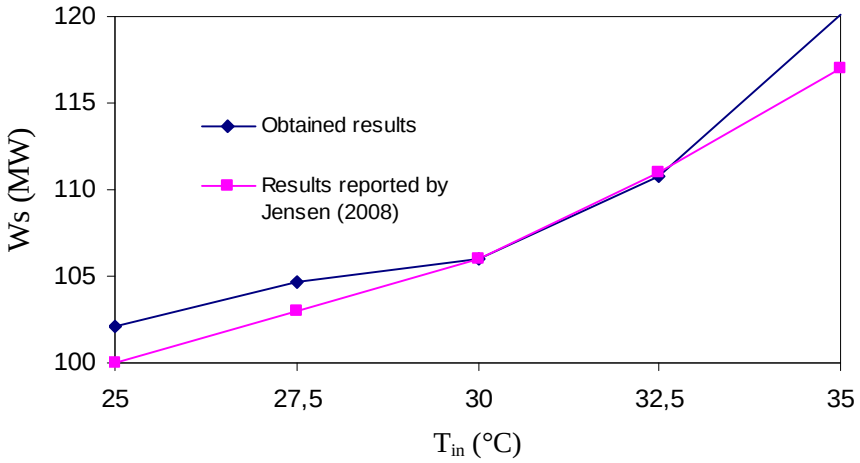

Figure 4.7. Mode I compressor work as a function of NG and MR temperatures

The reported results by Jensen (2008) seem to be more optimal than the ones obtained in this work (see Fig. 4.7). However, what is important to highlight is that both results present the same trend.

4.5.2 Mode II

- **Maximum compressor work (Ws^{max})**

In this section, we study how the production of LNG is influenced by the maximum compressor work. The results in Table 4.8 show that the LNG production increases by increasing the maximum compressor work. This is completely logical since there is more refrigerant that can be used by the compressor, and therefore more NG can be cooled. From Ws^{max} = 110 MW to Ws^{max} = 130 MW, the LNG production is increased in 15%. Note that it is always optimal to run the compressors at its maximal speed.

Table 4.8. Mode II optimal conditions with compressor work as disturbance

	Ws^{max} = 110 MW	Ws^{max} = 115 MW	Ws^{max} = 120 MW	Ws^{max} = 125 MW	Ws^{max} = 130 MW
$\dot{m}_{Ref}$ (Kg/s)	562.2	587.9	613.1	640.3	665.9
$\dot{m}_{LNG}$ (Kg/s)	71.28	74.77	77.88	81.17	84
P_h (bar)	26.53	28.07	29.51	31.35	33
P_l (bar)	4.264	4.388	4.5	4.627	4.73
N (rpm)	1000	1000	1000	1000	1000
η (%)	81.775	81.851	81.729	81.981	81.982

The dependence between the maximum compressor work and the LNG production is shown in Fig.4.8. In this graphic we can see that Jensen's curve also represents a growing tendency with a total increment of about 12.9%. Additionally, we have to note that computed results are more optimal than the ones reported by Jensen. This means we obtain higher LNG production for the same maximum compressor work.

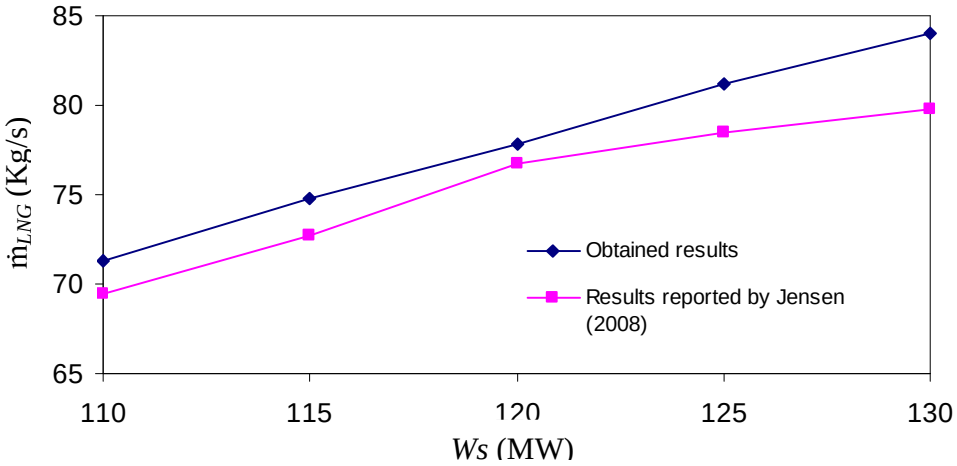

Figure 4.8. Mode II LNG flowrate as a function of compressor work

- **Natural gas feed temperature (T_{NG})**

We can note in the Table 4.9 and in the Fig.4.9 that the LNG production slightly decreases as increasing the NG temperature. As we can note the values for the process variables are not too difference between each other and specifically the LNG production only decreases in 1%, from T_{NG} =25°C to T_{NG} =35°C. This fact suggests that the optimum is a "flat" diagram in terms of NG temperature. Note that it is always optimal to run the compressors at maximum speed.

Table 4.9. Mode II optimal conditions with NG temperature as disturbance

	T_{NG} = 25 °C	T_{NG} = 27.5 °C	T_{NG} = 30 °C	T_{NG} = 32.5 °C	T_{NG} = 35 °C
$\dot{m}_{Ref}$ (Kg/s)	614.4	614.4	613.1	611.7	612.6
$\dot{m}_{LNG}$ (Kg/s)	78.55	78.38	77.88	77.83	77.78
P_h (bar)	29.8	29.77	29.51	29.78	29.77
P_l (bar)	4.5	4.506	4.5	4.53	4.532
N (rpm)	1000	1000	1000	1000	1000
η (%)	81.996	81.996	81.729	81.603	81.8

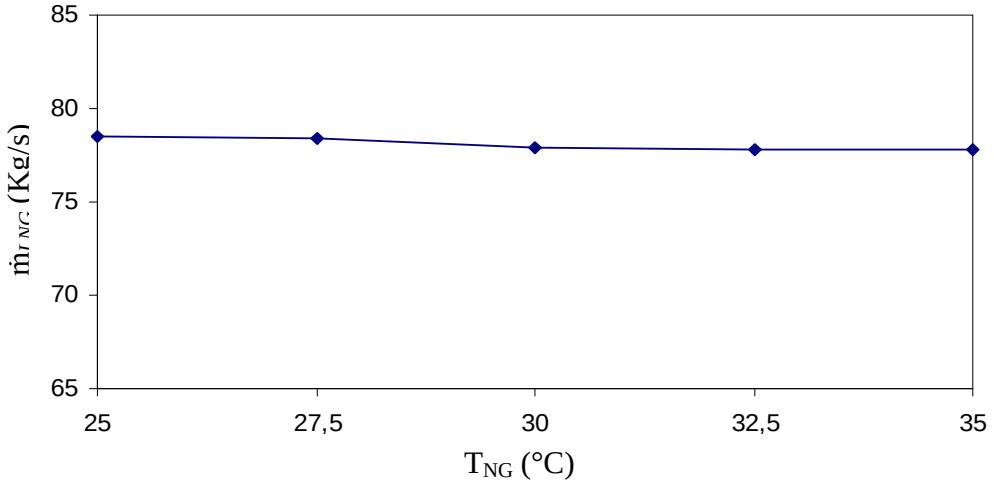

Figure 4.9. Mode II LNG flowrate as a function of NG temperature

- **Natural gas feed pressure (P_{NG})**

The computed results during the optimization with P_{NG} as disturbance are shown in Table 4.10. We can note that the LNG production increases while increasing the feed pressure. This is understandable because at high pressure the necessary cooling temperature is higher, so the natural gas can be cooled easier. The increment in LNG production is 6.6%, from P_{NG} = 35 bar to P_{NG} = 45.

Table 4.10. Mode II optimal conditions with NG pressure as disturbance

	P_{NG} = 35 bar	P_{NG} = 37.5 bar	P_{NG} = 40 bar	P_{NG} = 42.5 bar	P_{NG} = 45 bar
$\dot{m}_{Ref}$ (Kg/s)	615.3	614.2	613.1	614.6	613.9
$\dot{m}_{LNG}$ (Kg/s)	75.3	76.86	77.88	79.49	80.64
P_h (bar)	29.93	29.81	29.51	29.67	29.57
P_l (bar)	4.49	4.493	4.5	4.531	4.538
N (rpm)	1000	999.7	1000	1000	1000
η (%)	81.928	81.997	81.729	81.989	81.973

In the results presented by Jensen (2008) we can find a LNG increment of 6.4%, which is similar to the value we acquired. In the following Fig. 4.10 we can see that the LNG production curves have the same tendency.

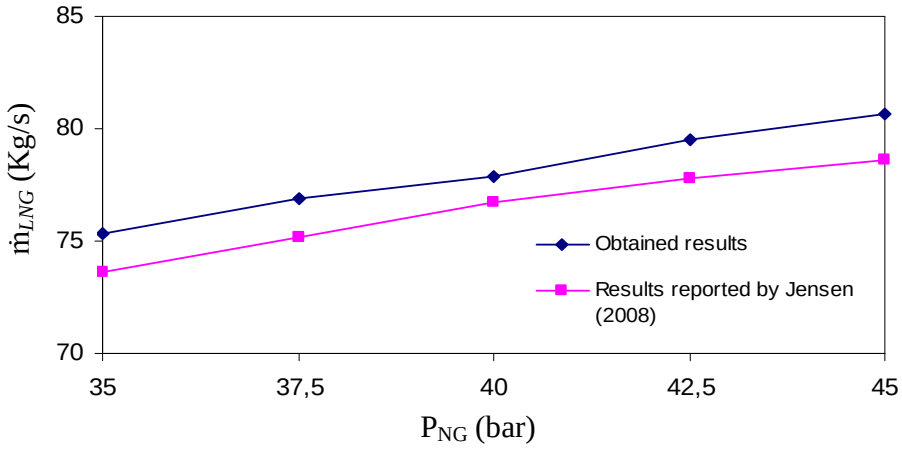

Figure 4.10. Mode II LNG flowrate as a function of NG pressure

- **Mixed refrigerant temperature after the SW cooler (T_7)**

As we should expect, the LNG production decreases by increasing the SW cooling temperature. This fact is shown by the computed results in Table 4.11. The reduction of LNG production is about 7.4%. Note that it is always optimal to run the compressor at its maximal speed.

Table 4.11: Mode II optimal conditions with MR temperature as disturbance

	T_7 = 27 °C	T_{NG} = 28.5 °C	T_{NG} = 30 °C	T_{NG} = 31.5 °C	T_{NG} = 33 °C
$\dot{m}_{Ref}$ (Kg/s)	614.6	611.9	613.1	612.2	613.4
$\dot{m}_{LNG}$ (Kg/s)	80.7	78.91	77.88	76.03	74.71
P_h (bar)	30.36	29.55	29.51	29.07	29.06
P_l (bar)	4.392	4.43	4.5	4.55	4.618
N (rpm)	1000	1000	1000	1000	1000
η (%)	81.998	81.435	81.729	81.503	81.815

Fig. 4.11 shows the relationship between the LNG production and the refrigerant temperature:

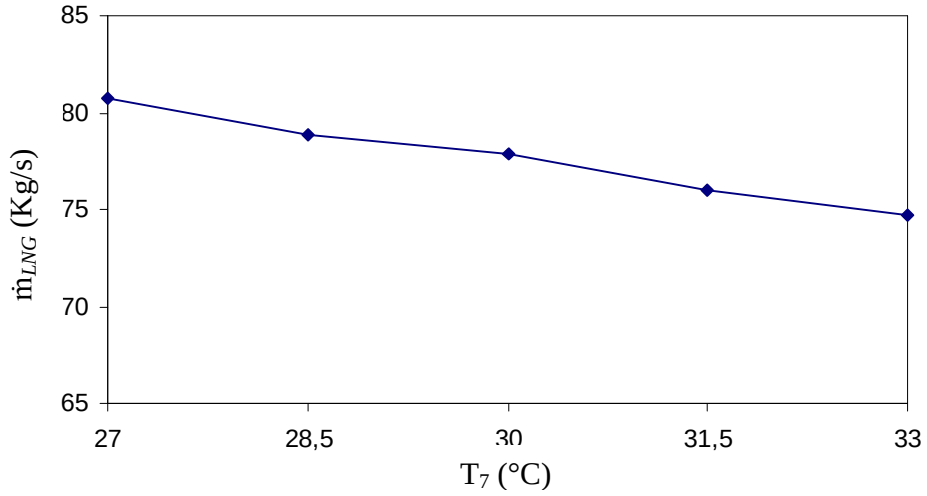

- **Temperature of the natural gas and mixed refrigerant at the inlet of the main heat exchanger (T_{in})**

As it is expected, the LNG production decreases while increasing the inlet temperature to the NG-HE. In this case, the LNG production decreased in about 12.6%. This change in the LNG production is the highest one for mode II. This means that the optimum value is strongly affected by the T_{in}. In the Table 4.12 we can see the optimal values for the process variables.

Table 4.12: Mode II optimal conditions with NG and MR temperature as disturbances

	T_{in} = 25 °C	T_{NG} = 27.5 °C	T_{NG} = 30 °C	T_{NG} = 32.5 °C	T_{NG} = 35 °C
$\dot{m}_{Ref}$ (Kg/s)	612	614.2	613.1	615.1	611.7
$\dot{m}_{LNG}$ (Kg/s)	82.4	80.51	77.88	75.3	72.04
P_h (bar)	30.98	30.28	29.51	29.29	28.93
P_l (bar)	4.299	4.401	4.5	4.625	4.726
N (rpm)	1000	1000	1000	1000	1000
η (%)	81.675	81.998	81.729	81.955	81.606

In the Figure 4.12 the LNG production is represented as function of T_{in}. The LNG increment for the Jensen's results is about 11.3%, which is similar to the one computed in this paper.

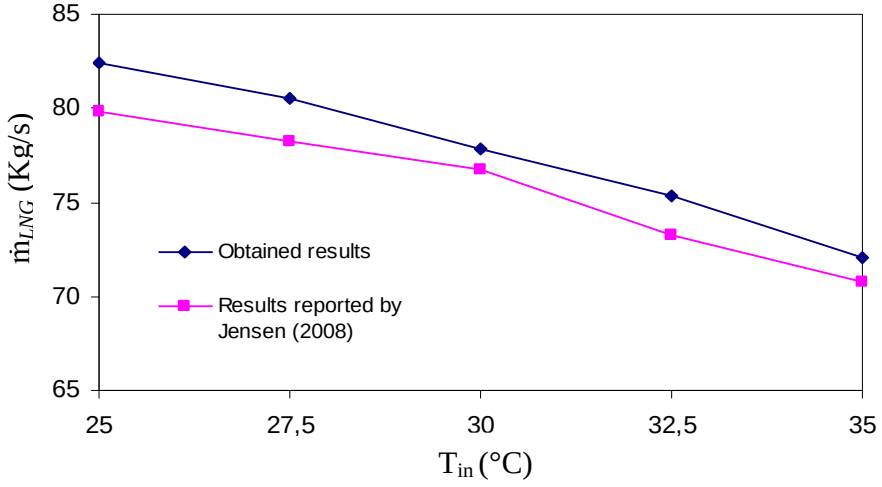

Figure 4.12. Mode II LNG flowrate as a function of NG and MR temperatures

While all the optimizations were being found, the optimal operation conditions were always given by a low pressure drop in VLV-101 (see Fig. 4.1). In most of the cases, the resulting pressure drop was equal to zero or was very close to it. That means it would be optimal to

remove VLV-101, and carry out all the refrigerant expansion in the turbine. This result is not surprising due to the fact that an isentropic expansion is more effective than an isenthalpic one (see section 2.1).

However, only using the liquid turbine is not applicable in real processes. If all the refrigerant expansion is finished in the turbine implies a high pressure drop and consequently, more vapor could be produced. The formed fraction of vapor might affect the liquid turbine's performance, even possibly damaging it. Furthermore, the only using a liquid turbine is not a common choice.

What is common is the use of a liquid turbine following an expansion valve. Thus the expansion process is made in two steps: first the refrigerant is expanded slightly above the saturation pressure and then the refrigerant pressure is reduced at the valve. In this way the vapor might be formed at the outlet of the valve but not in the liquid turbine.

Some cases were operating at the left side of maximum surge point (see Fig. 4.2). This means that even though HYSYS computes the different process variables, the results could not be applicable in practice. We tried to include a constraint for the compressor surge margin into the HYSYS 'optimizer', but we could not get a feasible solution.

4.6 Conclusions

By using the values of the total heat transfer area reported in Jensen's work (UA_{HOT} = 61.6 MW/°C), the HYSYS model was unable to satisfy the nominal conditions of the process. Specifically, the UA_{TOT} was not high enough to meet the nominal natural gas outlet temperature (T_{OUT} = -157 °C). Therefore, we had to compute a new value which matched the temperature specifications. The total obtained heat transfer area was equal to 63.56 MW/°C. This value was used for all the optimization studies.

The process operating in nominal Mode II, with the given compressor work equal to 120 MW, was optimized using two different refrigerant compositions. For both composition sets we got the same LNG production (77.88 Kg/s). This means that the optimal LNG production is stable for small refrigerant composition changes, when the process is operating in nominal Mode II.

The optimum nominal compressor work changed 15% while increasing the NG-HX inlet temperature (T_{in}) from 25 to 35 °C. This *Ws* variation was the highest change reported for the Mode I. Therefore we can conclude that for Mode I, T_{in} is the disturbance that affects the nominal optimum point the most. The optimum nominal LNG flowrate changed 12.6% while increasing the NG-HX inlet temperature (T_{in}) from 25 to 35 °C. This variation in the LNG production was the highest change reported for the Mode II. Thus we can conclude that for Mode II, T_{in} is the disturbance that affects the nominal optimum point the most.

The fed natural gas temperature (T_{NG}) was also introduced as a disturbance to the system. For Mode I, we observed that increasing T_{NG} from 25 to 35 °C only changed the optimum nominal compressor power by 0.5%. In Mode II, the optimum nominal LNG flowrate

changed 1% over the same temperature range. This means that the optimum nominal point is stable for natural gas temperature disturbances.

All the obtained results for the process optimum conditions are reasonable and match (at least in trend) well which the ones reported by Jensen (2008). Actually, in some cases the computed values in this work seem to provide better optimums: less compressor work for mode I and higher LNG production for mode II. From all this we can conclude that it is viable and advantageous to make process optimizations in the HYSYS simulator.

4.7 Future work

The process described in this work proved to be unstable for disturbances of T_7. The range of study for this variable (T_7 from 27.5 to 32.5 °C) was smaller than for the other temperatures because no feasible solutions were founded outside this range. It would be interesting to propose new refrigerant compositions and see if a feasible solution could be found for a wider temperature range.

The process operating in nominal Mode II showed to be stable for changes of refrigerant composition. Specifically, we got the same nominal optimum point using the reported MR composition for Mode II as using the same MR composition reported for Mode II. However, we do not know if the MR composition for Mode I could be kept as a constant for all the Mode II optimization cases. So, it would be interesting to do all the disturbance study for Mode II but using the MR composition of Mode I.

References

1) Energy Information Agency (EIA), Official Energy Statics from the US government.
Report #:DOE/EIA-0484(2008)
http://www.eia.doe.gov/oiaf/ieo/nat_gas.html

2) Norwegian Ministry of petroleum and energy
Norway's oil and gas resources
http://www.regjeringen.no/en/dep/oed/Subject/Oil-and-Gas/Norways-oil-and-gas-resources.html?id=443528

3) Black & Veatch publications
Patented PRICO® LNG Process a Deciding Factor in Selection of Black & Veatch Consortium for Project in Bali
http://www.bv.com/wcm/press_release/12042008_9064.aspx

4) Jensen, Jørgen B., 2008, "Optimal operation of refrigerant cycles", Doctoral thesis, Norwegian University of Science and technology.

5) Edgar, T.F., and Himmelblau, D.M., 1988, "Optimization of chemical process", McGraw-Hill, United States of America.

6) Nocedal, J., and Wright, S., 1999, "Numerical optimization", Springer series in operation research, United States of America.

7) Aspen HYSYS 2004.2 Operations Guide, AspenTech, 2004.

8) Jensen, Jørgen B., Skogestad, S.: Optimal operation of a simple LNG process, Adchem 2006

9) Kyle, B., 1984, "Chemical and process thermodymics", Pretince-Hall, 2nd edition, United States of America.

10) Sandler, S., 2006, "Chemical, Biochemical, and Engineering Thermodynamics", Wiley, fourth edition, United States of America.

11) Michot Michelle, 2007, "Introduction to LNG", Center for energy economics, The University of Texas at Austin, United States of America.
http://www.beg.utexas.edu/energyecon/lng/documents/CEE_INTRODUCTION_TO_LNG_FINAL.pdf

Nomenclature

P_h	Compression pressure (high pressure)
P_l	Expansion pressure (low pressure)
T_l	Evaporation temperature (low temperature)
T_h	Condensation temperature (high temperature)
ΔT_{sup}	Degree of super heating
ΔT_{sub}	Degree of sub cooling
COP	Coefficient of performance
COP_{carnot}	Coefficient of performance for ideal cycle (Carnot cycle)
Ws	Shaft compressor work
Q_l	Evaporation heat
Pr	Pressure ratio
$\dot{m}_r$	Reduced flow rate
N_r	Reduced rotational compressor speed
Ƞ	Compressor efficiency
N	Compressor rotational speed
D	Compressor diameter
$\dot{m}_{NG}$	Natural flow rate
$\dot{m}_{LNG}$	LNG flow rate
$\dot{m}_{Flash}$	Flash gas flow rate
$\dot{m}_{Ref}$	Refrigerant flow rate
T_{out}	NG temperature at the outlet of the main heat exchanger
Vsuc	Compressor suction volume

UA_{HOT}	Hot side heat transfer area
UA_{NG}	NG side heat transfer area
UA_{TOT}	Total heat transfer area

Appendix

A.1 Refrigerant composition reported by Jensen for 9 different design cases.

Case	6.1	6.2	6.3	6.4	6.5	6.6	6.7	6.8	6.9
x_{CH_4} [mole-%]	33.3	32.3	32.3	32.5	31.1	29.2	31.9	32.5	33.2
$x_{C_2H_6}$ [mole-%]	35.3	33.2	33.4	34.7	32.3	32.9	32.7	32.9	33.5
$x_{C_3H_8}$ [mole-%]	0.0	0.0	0.0	0.0	0.0	0.0	0.0	0.0	0.0
$x_{n-C_4H_{10}}$ [mole-%]	25.0	24.6	24.3	22.8	26.7	30.3	25.2	23.4	23.5
x_{N_2} [mole-%]	6.4	9.9	10.0	10.0	9.9	7.6	10.2	11.2	9.8

A.2 Optimal refrigerant compositions reported by Jensen for operation.

		Mode I	Mode II
x_{CH_4} [mole-%]	Methane in refrigerant	31.9	32.7
$x_{C_2H_6}$ [mole-%]	Ethane in refrigerant	35.2	34.3
$x_{C_3H_8}$ [mole-%]	Propane in refrigerant	**0.0**	**0.0**
$x_{n-C_4H_10}$ [mole-%]	nButane in refrigerant	24.7	23.3
x_{N_2} [mole-%]	Nitrogen in refrigerant	8.2	9.7